International Journal of Modern Physics E
© World Scientific Publishing Company

arXiv:0902.0125v1 [hep-ph] 1 Feb 2009

# DECONFINEMENT AND QUARK–GLUON PLASMA

A.V. NEFEDIEV, YU.A. SIMONOV, M.A. TRUSOV

*Institute of Theoretical and Experimental Physics, Russia 117218, Moscow, Bolshaya Cheremushkinskaya str. 25*

The theory of confinement and deconfinement is discussed as based on the properties of the QCD vacuum. The latter are described by field correlators of colour-electric and colour-magnetic fields in the vacuum, which can be calculated analytically and on the lattice. As a result one obtains a self-consistent theory of the confined region in the $(\mu, T)$ plane with realistic hadron properties. At the boundary of the confining region, the colour-electric confining correlator vanishes, and the remaining correlators describe strong nonperturbative dynamics in the deconfined region with (weakly) bound states. Resulting equation of state for $\mu = 0$, $p(T)$, $\frac{\varepsilon-3P}{T}$ are in good agreement with lattice data. Phase transition occurs due to evaporation of a part of the colour-electric gluon condensate, and the resulting critical temperatures $T_c(\mu)$ for different $n_f$ are in good correspondence with available data.

## Contents

**1 Introduction** **3**

**2 FCM at $T = 0$** **4**
- 2.1 Essentials of the method . . . . . . . . . . . . . . . . . . . . . . . . . 4
- 2.2 Colour-electric and colour-magnetic correlators . . . . . . . . . . . . 7
- 2.3 QCD string approach . . . . . . . . . . . . . . . . . . . . . . . . . . . 9
- 2.4 Spin-dependent interactions in hadrons . . . . . . . . . . . . . . . . . 11

**3 FCM at $T > 0$** **13**
- 3.1 The winding measure of integration . . . . . . . . . . . . . . . . . . . 13
- 3.2 Nonperturbative dynamics of quarks and gluons in the single-line approximation . . . . . . . . . . . . . . . . . . . . . . . . . . . . . . 14
- 3.3 Polyakov lines at finite temperatures . . . . . . . . . . . . . . . . . . 18
- 3.4 Equation of state . . . . . . . . . . . . . . . . . . . . . . . . . . . . . 24

**4 Beyond Single Line Approximation: Interacting quarks and gluons** **28**
- 4.1 Bound states at $T > T_c$ due to colour-electric forces . . . . . . . . . 29
- 4.2 Bound states at $T > T_c$ due to colour-magnetic forces . . . . . . . . 33

**5 Generalisation to nonzero baryon densities** **39**
- 5.1 Nonperturbative EoS for $\mu > 0$ . . . . . . . . . . . . . . . . . . . . . 39
- 5.2 Phase transition for nonzero $\mu$ . . . . . . . . . . . . . . . . . . . . . 41
- 5.3 Discussion of results . . . . . . . . . . . . . . . . . . . . . . . . . . . 44

**6 Concluding discussions** **45**
- 6.1 Comparison to other approaches . . . . . . . . . . . . . . . . . . . . . 45
- 6.2 Mysteries of deconfinement . . . . . . . . . . . . . . . . . . . . . . . . 48

## 1. Introduction

The fundamental problems of confinement and deconfinement have recently become a hot topic because of a possible observation of deconfined phase — the Quark-Gluon Plasma (QGP) at RHIC [1]. The theory of the QGP was mainly centered on perturbative ideas with an inclusion of some resummations and nonperturbative effects [2,3]. However, the experimental data [1] display a strong interacting QGP, with some properties more similar to a liquid, rather than to a weakly interacting plasma, with strong collective effects and large energy loss of fast constituents. These effects call for a nonperturbative treatment of QGP, and hence for a nonperturbative theory of confined and deconfined phases of QCD.

For the confined phase the corresponding methods have been suggested in [4] and formulated as the Field Correlator Method (FCM) — see [5] for a review. In the FCM at $T = 0$, the vacuum configurations support mostly two scalar quadratic in field correlators, $D(x)$ and $D_1(x)$. The first correlator is purely nonperturbative and ensures confinement, while the second one contains both perturbative and nonperturbative parts. As a result one obtains linear confining potential from the $D(x)$ plus perturbative and nonperturbative corrections coming from the $D_1(x)$. The spectra of all possible bound states (mesons, baryons, hybrids and glueballs) have been calculated in FCM, with current masses of quarks, the string tension $\sigma$, and the strong coupling constant $\alpha_s(\Lambda_Q)$ used as input, in good agreement with the experiment (see [6,7] for a review) and lattice data [8]. One can conclude therefore that the FCM describes well the confining region at $T = \mu = 0$.

For $T > 0$ several complications occur (see [9–12] for the details). First of all, colour-electric and colour-magnetic field correlators are no longer identical to each other and one has to do with five correlators instead of two: $D^E(x)$, $D_1^E(x)$, $D^H(x)$, $D_1^H(x)$, and $D_1^{EH}(x)$. Correspondingly, the colour-electric and colour-magnetic condensates are now different, as well as the string tensions, which are simply related to the correlators,

$$\sigma^{E(H)} = \frac{1}{2}\int D^{E(H)}(x)d^2x. \tag{1}$$

It is important to notice that only the electric tension $\sigma^E$ is responsible for confinement, while all others ensure spin-orbit forces. Thus it was conjectured in [9] that deconfinement occurs if the correlator $D^E(x)$ vanishes at $T = T_c(\mu)$. Indeed, this conjecture was confirmed later on the lattice, while all other correlators were measured to stay intact [8]. Finally, it was argued in [9] (see also [10]) that, since the vacuum energy density is proportional to the gluonic condensate, one can derive the condition of vanishing of the $D^E(0)$ directly from the second thermodynamic law. Consequently, general features of the phase transitions and the very value of the critical temperature $T_c(\mu)$ can be calculated in terms of the difference of the gluonic condensates in the confining and deconfining phases [9,11].

We now come to the central point of the paper: namely what is the dynamics of the QGP and its Equation of State (EoS)? As will be shown below, the basic role in the EoS is played by two effects: the colour-electric (nonconfining) forces due to the correlator $D_1^E(x)$ and colour-magnetic forces due to the correlator $D^H(x)$. The former one is dominant for $T_c \le T \le 1.5T_c$ and creates an effective mass (energy) of isolated quarks and gluons, thus leading to typical curves for the pressure $p(T)$ similar to those observed in lattice calculations. Furthermore, the same $D_1^E(x)$ generates potential $V_1(r)$ which is able to bind quarks and gluons [7,9], and provides strong correlations in white $3q$ systems. Colour-magnetic forces which stem from the $D^H(x)$ also can bind quarks at large distances and provide a large ratio $\langle$potential energy$\rangle/\langle$kinetic energy$\rangle \gtrsim 10$ specific for liquids [13]. Moreover, $D^H(x)$ (and thence $\sigma^H$) grow with the temperature, and finally become the basic interaction in the dimensionally reduced $3D$ QCD, with the transition temperature around $1.5 \div 2T_c$.

The paper is organised as follows. In Section 2 we introduce the FCM at $T = 0$. In particular, we give necessary essentials of the method, discuss colour-electric and colour-magnetic interactions, explain the QCD string approach to hadrons, and consider spin-dependent interactions. In Section 3 we generalise the FCM for nonzero temperatures: we introduce the winding measure of integration, define the Single Line Approximation (SLA), and derive the EoS of the QGP in the framework of the SLA. In Section 4 we discuss interactions between quarks and gluons above the $T_c$ and investigate bound states of quarks and gluons due to these interactions. In Section 5 we generalise the results of Section 3 for nonzero chemical potentials $\mu > 0$. In Section 6 we compare the results discussed in this review with other approaches found in the literature and discuss various solved and unsolved problems.

## 2. FCM at $T = 0$

### 2.1. *Essentials of the method*

To describe the dynamics of quarks and gluons in both confining and deconfined phases of QCD we start from the gauge-covariant Green's function of a single quark (or gluon) in the field of other quarks and gluons plus vacuum fields and use the Fock–Feynman–Schwinger Representation (FFSR) (in Euclidean space-time) [14]:

$$S(x,y|A) = \langle x|(m+\hat{D})^{-1}|y\rangle = (m-\hat{D})\int_0^\infty ds(Dz)_{xy}e^{-K}\Phi_\sigma(x,y,s) \qquad (2)$$

where $K$ is the kinetic energy term,

$$K = m^2 s + \frac{1}{4}\int_0^s d\tau\left(\frac{dz_\mu(\tau)}{d\tau}\right)^2, \qquad (3)$$

with $m$ being the pole mass of the quark. The parallel transporter along the trajectory $z_\mu(\tau)$ of the quark propagating from point $x$ to point $y$ is given by

$$\Phi(x,y) = P_A \exp\left[ig\int_y^x dz_\mu A_\mu\right], \qquad (4)$$

while

$$\Phi_\sigma(x,y,s) = \Phi(x,y) P_F \exp\left[ g \int_0^s \sigma_{\mu\nu} F_{\mu\nu}(z(\tau)) d\tau \right], \tag{5}$$

where

$$\sigma_{\mu\nu} = \frac{1}{4i}(\gamma_\mu\gamma_\nu - \gamma_\nu\gamma_\mu), \quad \sigma_{\mu\nu}F_{\mu\nu} \equiv \sigma F = \begin{pmatrix} \boldsymbol{\sigma H} & \boldsymbol{\sigma E} \\ \boldsymbol{\sigma E} & \boldsymbol{\sigma H} \end{pmatrix}, \tag{6}$$

and $\boldsymbol{\sigma}$ are the usual $2 \times 2$ Pauli matrices. The symbols $P_A$ and $P_F$ in (4) and (5) stand for the ordering operators for the matrices $A_\mu$ and $F_{\mu\nu}$, respectively, along the quark path.

Similarly, for one gluon Green's function, one writes

$$G_{\mu\nu}(x,y|A) = \langle x | (\tilde{D}^2_\lambda \delta_{\mu\nu} - 2ig\tilde{F}_{\mu\nu})^{-1} | y \rangle \tag{7}$$

and, proceeding in the same lines as for quarks, one arrives at the gluon Green's function in the FFSR:

$$G_{\mu\nu}(x,y|A) = \int_0^\infty ds (Dz)_{xy} e^{-K_0} \tilde{\Phi}_{\mu\nu}(x,y,s), \tag{8}$$

where

$$K_0 = \frac{1}{4}\int_0^\infty \left(\frac{dz_\mu}{d\tau}\right)^2 d\tau, \quad \tilde{\Phi}_{\mu\nu}(x,y,s) = \left[ \tilde{\Phi}(x,y) P_F \exp\left( 2g \int_0^s d\tau \tilde{F}(z(\tau)) \right) \right]_{\mu\nu}. \tag{9}$$

Here and below the tilde sign denotes quantities in the adjoint representation, for example, $\tilde{F}^{bc}_{\mu\nu} \equiv iF^a_{\mu\nu} f^{abc}$.

The single-quark(gluon) Green's functions (2) and (8) can be used now as building blocks to write the Green's function of a hadron. For example, for the quark–antiquark meson one has:

$$G_{q\bar{q}}(x,y|A) = \mathrm{Tr}(S_q(x,y|A)\Gamma S^\dagger_{\bar{q}}(x,y|A)\Gamma^\dagger), \tag{10}$$

where $\Gamma$ is a Dirac $4 \times 4$ matrix which provides the correct quantum numbers of the meson ($\Gamma$=1, $\gamma_\mu$, $\gamma_5$, $\gamma_\mu\gamma_5$, ...) and the trace is taken in both Dirac and colour indices. The next important step is building the physical Green's function of the meson,

$$G_{q\bar{q}}(x,y) = \langle G_{q\bar{q}}(x,y|A) \rangle_A, \tag{11}$$

where the averaging over gluonic fields is done with the usual Euclidean weight containing all gauge-fixing and ghost terms. The exact form of this weight is inessential for what follows.

The actual average one needs to evaluate in order to proceed reads:

$$\langle W_{\sigma_1\sigma_2}(C) \rangle = \langle \Phi(C) \Phi_{\sigma_1}(C,s_1) \Phi_{\sigma_2}(C,s_2) \rangle_A, \tag{12}$$

where the closed contour $C$ runs along the trajectories of the quark, $z_{1\mu}(\tau_1)$, and that of the antiquark, $z_{2\mu}(\tau_2)$. Since the orderings $P_A$ and $P_F$ in $\Phi_{\sigma_1}$, and $\Phi_{\sigma_2}$, are universal, then $W_{\sigma_1\sigma_2}(C)$ is just a Wegner–Wilson loop with the insertion of the operators $(\sigma_1 F)$ and $(\sigma_2 F)$ at proper places along the contour $C$.

To proceed it is convenient to rewrite (12) in the form

$$\langle W_{\sigma\sigma'}(C)\rangle = \left\langle \exp ig\int_S d\pi_{\mu\nu}(z)F_{\mu\nu}(z)\right\rangle, \tag{13}$$

where the non-Abelian Stokes theorem [15] was used and the integral is taken over the surface $S$ bounded by the contour $C$. Notice that the differential

$$d\pi_{\mu\nu}(z) = ds_{\mu\nu}(z) - i\sigma^{(1)}_{\mu\nu}d\tau_1 + i\sigma^{(2)}_{\mu\nu}d\tau_2 \tag{14}$$

contains not only the surface element $ds_{\mu\nu}$ but it also incorporates the spin variables. This is the most economical way to include into consideration spin-dependent interactions between quarks ($\tau_1$ and $\tau_2$ are the proper-time variables for the quark and the antiquark, respectively). Furthermore, if a cluster expansion theorem is applied to the right-hand side of (13), then the result reads:

$$\frac{1}{N_C}\langle W_{\sigma_1\sigma_2}(C)\rangle = \exp\sum_{n=1}^{\infty}\frac{(ig)^n}{n!}\int d\pi(1)\ldots\int d\pi(n)\langle\langle F(1)\ldots F(n)\rangle\rangle, \tag{15}$$

where $d\pi(k)\equiv d\pi_{\mu_k\nu_k}(z)$ and $F(k)\equiv F_{\mu_k\nu_k}(u_k,x_0)\equiv\Phi(x_0,u_k)F_{\mu_k\nu_k}(u_k)\Phi(u_k,x_0)$. Double brackets $\langle\langle\ldots\rangle\rangle$ denote irreducible (connected) averages, and the reference point $x_0$ is arbitrary.

Equation (15) is exact and therefore its right-hand side does not depend on any particular choice of the surface $S$. At this step one can make the first approximation by keeping only the lowest (quadratic, or Gaussian) field correlator $\langle\langle FF\rangle\rangle$, while the surface is chosen to be the minimal area surface. As it was argued in [16], using comparison with lattice data, this approximation (sometimes called the Gaussian approximation) has the accuracy of a few per cent.

As was mentioned before, the factors $(m-\hat{D})$ in the Green's function (11) need a special treatment in the process of averaging over the gluonic fields — it is shown in [17] that one can use a simple replacement,

$$m-\hat{D}\to m-i\hat{p},\quad p_\mu = \frac{1}{2}\left(\frac{dz_\mu}{d\tau}\right)_{\tau=s}. \tag{16}$$

Therefore, the first step is fulfilled, namely the derivation of the physical Green's function of a quark–antiquark meson (one can proceed along the same lines for baryons and hadrons with an excited glue) in terms of the vacuum correlator $\langle\langle FF\rangle\rangle$. In the next chapter the structure of this Gaussian correlator is studied, in particular, its separation into colour-electric and colour-magnetic parts.

### 2.2. *Colour-electric and colour-magnetic correlators*

The Gaussian correlator of background gluonic fields can be parameterized via two scalar functions, $D$ and $D_1$ [4]:

$$\begin{aligned}\langle\langle FF\rangle\rangle \equiv D_{\mu\nu\lambda\rho}(z-z') &= \frac{g^2}{N_c}\langle\langle \mathrm{Tr}F_{\mu\nu}(z)\Phi(z,z')F_{\lambda\rho}(z')\Phi^\dagger(z,z')\rangle\rangle \qquad (17)\\ &= (\delta_{\mu\lambda}\delta_{\nu\rho}-\delta_{\mu\rho}\delta_{\nu\lambda})D(u)+\frac{1}{2}\left[\frac{\partial}{\partial u_\mu}(u_\lambda\delta_{\nu\rho}-u_\rho\delta_{\lambda\nu})+\begin{pmatrix}\mu\leftrightarrow\nu\\ \lambda\leftrightarrow\rho\end{pmatrix}\right]D_1(u),\end{aligned}$$

where $u=z-z'$. Notice that, in order to proceed from (15) to (17) one needs to show that, for the correlators in (15) taken at close points, $|z-z'|\lesssim T_g$[a], the parallel transporters $\Phi$ passing through the point $x_0$ can be reduced to the straight line between the points $z$ and $z'$. To this end, notice that, for a generic configuration with $|z-z'|\ll|z-x_0|,|z'-x_0|\sim R$ ($R$ is the radius of the Wilson loop, of order of the hadron size), one can write $\Phi(z-x_0)\Phi(x_0-z')\approx\Phi(z-z')+O(T_g^2/R^2)$.

For future convenience let us also write the correlator (17) in components:

$$\begin{aligned}\frac{g^2}{N_c}\langle\langle \mathrm{Tr}E_i(z)\Phi E_j(z')\Phi^\dagger\rangle\rangle &= \delta_{ij}\left[D^E(u)+D_1^E(u)+u_4^2\frac{\partial D_1^E}{\partial u^2}\right]+u_iu_j\frac{\partial D_1^E}{\partial u^2},\\ \frac{g^2}{N_c}\langle\langle \mathrm{Tr}H_i(z)\Phi H_j(z')\Phi^\dagger\rangle\rangle &= \delta_{ij}\left[D^H(u)+D_1^H(u)+\boldsymbol{u}^2\frac{\partial D_1^H}{\partial \boldsymbol{u}^2}\right]-u_iu_j\frac{\partial D_1^H}{\partial u^2}, \qquad (18)\\ \frac{g^2}{N_c}\langle\langle \mathrm{Tr}H_i(z)\Phi E_j(z')\Phi^\dagger\rangle\rangle &= \varepsilon_{ijk}u_4u_k\frac{\partial D_1^{EH}}{\partial u^2}.\end{aligned}$$

For the sake of brevity we omit, in this chapter, the spin-dependent terms in the Wilson loop (15) and consider only nonperturbative contributions to the Gaussian correlator $\langle\langle FF\rangle\rangle$ responsible for confinement and given by the correlator $D$. This correlator enters the Wilson loop (15) multiplied by the surface elements $ds_{\mu\nu}ds_{\lambda\rho}$ and, in what follows, we distinguish between the colour-electric and colour-magnetic contributions in (18). The former are accompanied by the structure $ds_{0i}ds_{0i}$ and enters (15) multiplied by electric correlator $D^E$, whereas, for the latter, these are $ds_{jk}ds_{jk}$ and $D^H$, respectively. The electric and magnetic string tensions are defined then according to (1).

We now proceed from the proper-time variables to the laboratory times by performing the following change of variables:

$$d\tau_1=\frac{dz_{10}}{2\mu_1},\quad d\tau_2=\frac{dz_{20}}{2\mu_2} \qquad (19)$$

and synchronise the quarks in the laboratory frame, putting $z_{10}=z_{20}=t$. The new variables $\mu_{1,2}$ which appeared in (19) are known as the auxiliary (or einbein) fields [20,21,22]. The physical meaning and the role played by the einbeins will be discussed in detail below. Now we can write the surface element through the string profile function $w_\mu(t,\beta)$ as

---

[a] The gluonic correlation length $T_g$ defines the distance at which the background gluonic fields are correlated or, more specifically, the correlator $D(u)$ defined in (17) decreases in all directions of the Euclidean space, and the length $T_g$ governs this decrease. The correlation length $T_g$ extracted from the lattice data is quite small, $T_g\lesssim 0.1$ fm [18,19].

$$ds_{\mu\nu}(z)=\varepsilon^{ab}\partial_a w_\mu(t,\beta)\partial_b w_\nu(t,\beta)dtd\beta,\quad \{a,b\}=\{t,\beta\},\tag{20}$$

where $0\leqslant t\leqslant t_{\max}$, $0\leqslant\beta\leqslant 1$, and we adopt the straight–line ansatz for the minimal string profile, so that the latter is defined by the trajectories of the quarks [21]:

$$w_\mu(t,\beta)=\beta z_{1\mu}(t)+(1-\beta)z_{2\mu}(t).\tag{21}$$

For further convenience let us introduce two vectors:

$$\boldsymbol{r}=\boldsymbol{z}_1-\boldsymbol{z}_2,\quad \boldsymbol{\rho}=[(\boldsymbol{z}_1-\boldsymbol{z}_2)\times(\beta\dot{\boldsymbol{z}}_1+(1-\beta)\dot{\boldsymbol{z}}_2)]\equiv r\boldsymbol{\omega},\tag{22}$$

where $\boldsymbol{\omega}$ is the angular rotation vector. This allows one to write the differentials in a compact form,

$$ds_{0i}(z)ds_{0i}(z')=\boldsymbol{r}(t)\boldsymbol{r}(t')dtdt'd\beta d\beta',\quad ds_{jk}(z)ds_{jk}(z')=2\boldsymbol{\rho}(t)\boldsymbol{\rho}(t')dtdt'd\beta d\beta'.\tag{23}$$

Presenting the averaged Wilson loop (15) (without spins) as

$$\frac{1}{N_C}\langle TrW(C)\rangle=e^{-J},\quad J=J^E+J^H,$$

one can write for the electric and magnetic contributions separately:

$$J^E=\int_0^{t_{\max}}dt\,dt'\int_0^1 d\beta\,d\beta'\,\boldsymbol{r}(t)\boldsymbol{r}(t')D^E(z-z'),\tag{24}$$

$$J^H=\int_0^{t_{\max}}dt\,dt'\int_0^1 d\beta\,d\beta'\,\boldsymbol{\rho}(t,\beta)\boldsymbol{\rho}(t',\beta')D^H(z-z').\tag{25}$$

The correlation functions $D^{E,H}$ decrease in all directions of the Euclidean space–time with the correlation length $T_g$ which is measured on the lattice to be rather small, $T_g\approx 0.2\div 0.3$ fm [8] or even smaller, $T_g\lesssim 0.1$ fm [18,19]. Therefore, only close points $z$ and $z'$ are correlated, so that one can neglect the difference between $\boldsymbol{r}(t)$ and $\boldsymbol{r}(t')$, $\boldsymbol{\rho}(t,\beta)$ and $\boldsymbol{\rho}(t',\beta')$ in (24), (25) and also write:

$$(z-z')^2=(z(t,\beta)-z(t',\beta'))^2=g^{ab}\xi_a\xi_b,\quad \xi_a=t-t',\quad \xi_b=\beta-\beta'.\tag{26}$$

The induced metric tensor is $g^{ab}=g^a\delta^{ab}$, $g^1g^2=det\ g=r^2+\rho^2=r^2(1+\omega^2)$. Now, after an appropriate change of variables and introducing the string tensions, according to (1), one readily finds:

$$J^E=\sigma_E\int_0^{t_{\max}}dt\int_0^1 d\beta\frac{r^2}{\sqrt{r^2+\rho^2}}=\sigma_E r\int_0^{t_{\max}}dt\int_0^1 d\beta\frac{1}{\sqrt{1+\omega^2}},\tag{27}$$

$$J^H=\sigma_H\int_0^{t_{\max}}dt\int_0^1 d\beta\frac{\rho^2}{\sqrt{r^2+\rho^2}}=\sigma_H r\int_0^{t_{\max}}dt\int_0^1 d\beta\frac{\omega^2}{\sqrt{1+\omega^2}}.\tag{28}$$

For $\sigma_E = \sigma_H = \sigma$ the sum of $J^E$ and $J^H$ reproduces the well-known action of the Nambu–Goto string (see, for example, [20–22]),

$$J = J^E + J^H = \sigma r \int_0^{t_{\max}} dt \int_0^1 d\beta \sqrt{1+\omega^2}. \tag{29}$$

Notice that, for $\omega \ll 1$, $J_E = \sigma_E r \times t_{\max} + O(\omega^2)$ and $J_H = O(\omega^2)$, that is confinement is of a purely colour-electric nature while the colour-magnetic contribution is entirely due to the rotation of the system.

### 2.3. *QCD string approach*

With the form of the colour-electric and colour-magnetic spin-independent interactions (27) and (28) in hand we are in a position to build a quantum-mechanical model of hadron consisting of quarks (gluons) connected by straight-line Nambu-Goto strings. Below we consider, as a paradigmatic case, a quark–antiquark meson.

We start from the kinetic energies of the quarks,

$$K_i = m_i^2 s_i + \frac{1}{4}\int_0^{s_i} d\tau_i \left(\frac{dz_{i\mu}(\tau_i)}{d\tau_i}\right)^2 = \int_0^{t_{\max}} dt \left[\frac{m_i^2}{2\mu_i} + \frac{\mu_i}{2} + \frac{\mu_i \dot{\boldsymbol{z}}_i^2}{2}\right], \quad i = 1, 2, \tag{30}$$

where (19) was used, and path integrals in $\mu_i$ appear through the substitution $ds_i Dz_{i0} \to D\mu_i$. One can see therefore that the einbeins should be treated on equal footings with other coordinates. However, since time derivatives of the einbeins, $\dot{\mu}_i$, do not enter (30), they can be eliminated with the help of the well-known integral:

$$\int D\mu \exp\left[-\int_0^{t_{\max}} \left(\frac{a\mu}{2} + \frac{b}{2\mu}\right) dt\right] \sim \exp\left[-\int_0^{t_{\max}} \sqrt{ab}\, dt\right]. \tag{31}$$

Then, with the help of (2), (27), (28), and (30), one can extract the Lagrangian of the quark–antiquark system in the form (notice that hereinafter in this chapter we work in Minkowski space-time):

$$L = -m_1\sqrt{1-\dot{\boldsymbol{z}}_1^2} - m_2\sqrt{1-\dot{\boldsymbol{z}}_2^2} - \sigma_E r \int_0^1 d\beta \frac{1}{\sqrt{1-[\boldsymbol{n}\times(\beta\dot{\boldsymbol{z}}_1 + (1-\beta)\dot{\boldsymbol{z}}_2)]^2}}$$

$$+\sigma_H r \int_0^1 d\beta \frac{[\boldsymbol{n}\times(\beta\dot{\boldsymbol{z}}_1 + (1-\beta)\dot{\boldsymbol{z}}_2)]^2}{\sqrt{1-[\boldsymbol{n}\times(\beta\dot{\boldsymbol{z}}_1 + (1-\beta)\dot{\boldsymbol{z}}_2)]^2}}, \quad \boldsymbol{n} = \frac{\boldsymbol{r}}{r}. \tag{32}$$

In fact, the einbein form of the kinetic energies is much more convenient [20–22,23] since it does not contain square roots (unbearable for path integrals) and one deals with formally nonrelativistic kinetic terms, while the entire set of relativistic corrections is summed by taking extrema in the einbeins. Furthermore, extra (continuous) einbeins, $\nu(\beta)$ and $\eta(\beta)$, can be introduced in order to simplify the string terms in (32), through the substitutions:

$$\int_0^1 d\beta\sqrt{AB} \to \int_0^1 d\beta \left(\frac{A}{2\nu} + \frac{B\nu}{2}\right), \quad \int_0^1 d\beta \frac{A^2}{B} \to -\int_0^1 d\beta \left(B\eta^2 + 2A\eta\right). \tag{33}$$

Then, introducing the centre-of-mass position and the relative coordinate as

$$\boldsymbol{R}=\zeta_1\boldsymbol{x}_1+(1-\zeta_1)\boldsymbol{x}_2,\quad \boldsymbol{r}=\boldsymbol{x}_1-\boldsymbol{x}_2,\quad \zeta_1=\frac{\mu_1+\int_0^1\beta\nu d\beta}{\mu_1+\mu_2+\int_0^1\nu d\beta},\quad \zeta_2=1-\zeta_1, \tag{34}$$

one can rewrite the Lagrangian in the form (the centre-of-mass motion is omitted for simplicity):

$$L=-\sum_{i=1}^2\left[\frac{m_i^2}{2\mu_i}+\frac{\mu_i}{2}\right]-\int_0^1 d\beta\left(\frac{\sigma_1^2r^2}{2\nu}+\frac{\nu}{2}+\sigma_2 r\right)+\frac{1}{2}\mu(\dot{\boldsymbol{r}}\boldsymbol{n})^2+\frac{1}{2}\tilde{\mu}[\dot{\boldsymbol{r}}\times\boldsymbol{n}]^2, \tag{35}$$

where $\sigma_1=\sigma_H+\eta^2(\sigma_H-\sigma_E)$, $\sigma_2=2\eta(\sigma_E-\sigma_H)$ and we have defined the reduced masses for the angular and radial motion separately:

$$\mu=\frac{\mu_1\mu_2}{\mu_1+\mu_2}, \tag{36}$$

$$\tilde{\mu}=\mu_1(1-\zeta_1)^2+\mu_2\zeta_1^2+\int_0^1(\beta-\zeta_1)^2\nu d\beta. \tag{37}$$

The original form of the Lagrangian is readily restored once extrema in all four einbeins, $\{\mu_1,\mu_2,\nu(\beta),\eta(\beta)\}$, are taken. Generally speaking, the einbein fields appear in the Lagrangian and, as was mentioned before, even in absence of the corresponding velocities, they can be considered as extra degrees of freedom introduced to the system. The einbeins can be touched upon when proceeding from the Lagrangian of the system to its Hamiltonian and thus they mix with the ordinary particles coordinates and momenta. Besides, in order to preserve the number of physical degrees of freedom, constrains are to be imposed on the system and then the formalism of constrained systems quantisation [24] is operative (see, for example, [22] for the open straight–line QCD string quantisation using this formalism). A nontrivial algebra of constraints and the process of disentangling the physical degrees of freedom and non-physical ones make the problem very complicated. In the meantime, a simpler approach to einbeins exists which amounts to considering all (or some) of them as variational parameters and thus to taking extrema in the einbeins either in the Hamiltonian or in its spectrum [23,25]. Being an approximate approach this technique appears accurate enough (see, for example, [26]) providing a simple but powerful and intuitive method of investigation. The physical meaning of the variables $\mu_i$ ($i=1,2$) is the average kinetic energy of the $i$-th particle in the given state, namely, $\mu_i=\langle\sqrt{\boldsymbol{p}^2+m_i^2}\rangle$ (see the discussion in [21,26]). The continuous einbein variable $\nu(\beta)$ has the meaning of the QCD string energy density [21].

Following the standard procedure, we build now the canonical momentum as

$$\boldsymbol{p}=\frac{\partial L}{\partial\dot{\boldsymbol{r}}}=\mu(\boldsymbol{n}\dot{\boldsymbol{r}})\boldsymbol{n}+\tilde{\mu}(\dot{\boldsymbol{r}}-\boldsymbol{n}(\boldsymbol{n}\dot{\boldsymbol{r}})), \tag{38}$$

with its radial component and transverse component being

$$(\boldsymbol{n}\boldsymbol{p})=\mu(\boldsymbol{n}\dot{\boldsymbol{r}}),\quad [\boldsymbol{n}\times\boldsymbol{p}]=\tilde{\mu}[\boldsymbol{n}\times\dot{\boldsymbol{r}}], \tag{39}$$

respectively. Thus we arrive at the spin-independent part of the Hamiltonian [21]:

$$H = \sum_{i=1}^{2}\left[\frac{m_i^2}{2\mu_i}+\frac{\mu_i}{2}\right]+\int_0^1 d\beta\left(\frac{\sigma_1^2 r^2}{2\nu}+\frac{\nu}{2}+\sigma_2 r\right)+\frac{p_r^2}{2\mu}+\frac{\boldsymbol{L}^2}{2\tilde{\mu}r^2}. \qquad (40)$$

Notice that the kinetic part of the Hamiltonian (40) has a very clear structure: the radial motion of the quarks happens with the effective mass $\mu$, whereas for the orbital motion the mass $\tilde{\mu}$ is somewhat different, containing the contribution of the inertia of the string. For $\sigma_E = \sigma_H = \sigma$, the field $\eta$ drops from the Hamiltonian and the standard expression for the string with quarks at the ends [21] readily comes out from (40).

### 2.4. *Spin-dependent interactions in hadrons*

In heavy quarkonia (up to the order $1/m^2$) the standard Eichten–Feinberg decomposition is valid [27,28,29]:

$$\begin{aligned} V_{SD}^{(0)}(r) &= \left(\frac{\boldsymbol{\sigma}_1\boldsymbol{L}}{4m_1^2}+\frac{\boldsymbol{\sigma}_2\boldsymbol{L}}{4m_2^2}\right)\left[\frac{1}{r}\frac{dV_0}{dr}+\frac{2}{r}\frac{dV_1}{dr}\right]+\frac{(\boldsymbol{\sigma}_1+\boldsymbol{\sigma}_2)\boldsymbol{L}}{2m_1m_2}\frac{1}{r}\frac{dV_2}{dr} \\ &+\frac{(3(\boldsymbol{\sigma}_1\boldsymbol{n})(\boldsymbol{\sigma}_2\boldsymbol{n})-\boldsymbol{\sigma}_1\boldsymbol{\sigma}_2)}{12m_1m_2}V_3(r)+\frac{\boldsymbol{\sigma}_1\boldsymbol{\sigma}_2}{12m_1m_2}V_4(r), \end{aligned} \qquad (41)$$

where each potential $V_n(r)$ ($n$ =0-4) contains both perturbative (P) and nonperturbative (NP) contributions: $V_n(r) = V_n^P(r) + V_n^{NP}(r)$. The static interquark potential $V_0(r)$, together with the potentials $V_1(r)$ and $V_2(r)$, satisfies the Gromes relation [30],

$$V_0'(r)+V_1'(r)-V_2'(r)=0. \qquad (42)$$

Notice that this relation refers both to the perturbative and nonperturbative parts of the potentials $V_n(r)$ $(n = 0, 1, 2)$.

We now return to the Green's function of the quark–antiquark system (2) and restore spin–dependent terms in order to derive the generalisation of (41).

Let us quote here without derivation the full set of spin-dependent potentials, both perturbative and nonperturbative, obtained in the framework of FCM and with the string rotation taken into account (an interested reader can find the details of the derivation in [31]):

$$\begin{aligned}
&\left(\frac{\boldsymbol{\sigma}_1\boldsymbol{L}}{4\bar{m}_1^2}+\frac{\boldsymbol{\sigma}_2\boldsymbol{L}}{4\bar{m}_2^2}\right)\frac{1}{r}\frac{dV_0}{dr}\to\frac{1}{2r}\int_0^\infty d\nu\int_0^r d\lambda\left[D+D_1+(\lambda^2+\nu^2)\frac{\partial D_1}{\partial\nu^2}\right]\\
&\qquad\qquad\qquad\qquad\times\left[(1-\zeta_1)\frac{\boldsymbol{\sigma}_1\boldsymbol{L}}{\mu_1\tilde{\mu}}+(1-\zeta_2)\frac{\boldsymbol{\sigma}_2\boldsymbol{L}}{\mu_2\tilde{\mu}}\right],\\
&\left(\frac{\boldsymbol{\sigma}_1\boldsymbol{L}}{4\bar{m}_1^2}+\frac{\boldsymbol{\sigma}_2\boldsymbol{L}}{4\bar{m}_2^2}\right)\frac{2}{r}\frac{dV_1}{dr}\to-\frac{1}{r}\int_0^\infty d\nu\int_0^r d\lambda D\left(1-\frac{\lambda}{r}\right)\\
&\qquad\qquad\qquad\qquad\times\left[(1-\zeta_1)\frac{\boldsymbol{\sigma}_1\boldsymbol{L}}{\mu_1\tilde{\mu}}+(1-\zeta_2)\frac{\boldsymbol{\sigma}_2\boldsymbol{L}}{\mu_2\tilde{\mu}}\right],\\
&\frac{(\boldsymbol{\sigma}_1+\boldsymbol{\sigma}_2)\boldsymbol{L}}{2\bar{m}_1\bar{m}_2}\frac{1}{r}\frac{dV_2}{dr}\to\frac{1}{r^2}\int_0^\infty d\nu\int_0^r \lambda d\lambda\left[D+D_1+\lambda^2\frac{\partial D_1}{\partial\lambda^2}\right]\frac{(\boldsymbol{\sigma}_1+\boldsymbol{\sigma}_2)\boldsymbol{L}}{\tilde{\mu}}\left(\frac{\zeta_1}{\mu_1}\right),\\
&\frac{(3(\boldsymbol{\sigma}_1\boldsymbol{n})(\boldsymbol{\sigma}_2\boldsymbol{n})-\boldsymbol{\sigma}_1\boldsymbol{\sigma}_2)}{12\bar{m}_1\bar{m}_2}V_3(r)\to-2r^2\frac{\partial}{\partial r^2}\int_0^\infty d\nu D_1(r,\nu)\frac{(3(\boldsymbol{\sigma}_1\boldsymbol{n})(\boldsymbol{\sigma}_2\boldsymbol{n})-\boldsymbol{\sigma}_1\boldsymbol{\sigma}_2)}{12\mu_1\mu_2},\\
&\frac{\boldsymbol{\sigma}_1\boldsymbol{\sigma}_2}{12\bar{m}_1\bar{m}_2}V_4(r)\to 6\int_0^\infty d\nu\left[D(r,\nu)+\left[1+\frac{2}{3}r^2\frac{\partial}{\partial\nu^2}\right]D_1(r,\nu)\right]\frac{\boldsymbol{\sigma}_1\boldsymbol{\sigma}_2}{12\mu_1\mu_2},
\end{aligned}\tag{43}$$

where the masses $m_i$ are replaced by $\mu_i$ and $\tilde{\mu}$, which makes this result applicable also to light quarks. Notice that this result [32,6], is not due to the $1/m$ expansion, but is obtained with the only approximation made being the Gaussian approximation for field correlators (corrections may come from triple and quartic correlators). Accuracy of this approximation was checked both at $T=0$ [16] and at $T>T_c$ [33] to be of the order of one percent.

With this explicit form of the potentials and taking the limit of heavy quarks one can check the Gromes relation (42), which now reads:

$$\begin{aligned}
V_0'(r)+V_1'(r)-V_2'(r)=2\int_0^\infty d\nu\int_0^r d\lambda[D^E(\lambda,\nu)-D^H(\lambda,\nu)]\\
+r\int_0^\infty d\nu[D_1^E(r,\nu)-D_1^H(r,\nu)].
\end{aligned}\tag{44}$$

At $T=0$, $D^E=D^H$ and $D_1^E=D_1^H$, so that the Gromes relation (42) is satisfied. In the next Section we shall discuss the FCM at nonzero temperatures, in particular at $T>T_c$, where the latter equalities between colour-electric and colour-magnetic correlators do not hold, and the Gromes relation is therefore violated.

## 3. FCM at $T > 0$

### 3.1. *The winding measure of integration*

Now we turn to the case $T > 0$ and use Matsubara technique for the path integrals in the FFSR, first introduced in [12],

$$(Dz)^w_{xy} = \lim_{N\to\infty} \prod_{m=1}^{N} \frac{d^4\xi(m)}{(4\pi\varepsilon)^2} \times \sum_{n=0,\pm1,\ldots} \frac{d^4p}{(2\pi)^4} \exp\left[ip\left(\sum_{m=1}^{N} \zeta(m) - (x-y) - n\beta\delta_{\mu4}\right)\right]. \quad (45)$$

where $\zeta(k) = z(k) - z(k-1)$ and $\varepsilon = t/N$, and $\beta = 1/T$. It is easy to check that, with such a measure, for example, the free massless propagator takes its standard form:

$$\begin{aligned}(-\partial^2)^{-1}_{xy} &= \int_0^\infty dt \exp\left[-\sum_{m=1}^{N} \frac{\zeta^2(m)}{4\varepsilon}\right] \prod_m \frac{d\zeta(m)}{(4\pi\varepsilon)^2} \sum_n \frac{d^4p}{(2\pi)^4} \\ &\times \exp\left[ip\left(\sum \zeta(m) - (x-y) - n\beta\delta_{\mu4}\right)\right] \\ &= \sum_n \int_0^\infty \exp\left[-p^2t - ip(x-z) - ip_4n\beta\right] dt \frac{d^4p}{(2\pi)^4} \\ &= \sum_{k=0,\pm1,\ldots} \int \frac{Td^3p}{(2\pi)^3} \frac{\exp[-ip_i(x-y)_i - i2\pi kT(x_4-y_4)]}{p_i^2 + (2\pi kT)^2},\end{aligned} \quad (46)$$

where the Poisson summation formula was used to obtain:

$$\sum_{n=0,\pm1,\ldots} \exp(ip_4n\beta) = \sum_{k=0,\pm1,\ldots} 2\pi\delta(p_4\beta - 2\pi k). \quad (47)$$

For quarks one is to take into account the antisymmetric nature of the fermionic fields, which yields instead of (45)

$$\overline{(Dz)}^w_{xy} = \lim_{N\to\infty} \prod_{m=1}^{N} \frac{d^4\zeta(m)}{(4\pi\varepsilon)^2} \times \sum_{n=0,\pm1,\ldots} (-1)^n \frac{d^4p}{(2\pi)^4} \exp\left[ip\left(\sum_{m=1}^{N} \zeta(m) - (x-y) - n\beta\delta_{\mu4}\right)\right]. \quad (48)$$

Therefore, in order to proceed from $T = 0$ to $T > 0$ we simply replace $(Dz)_{xy}$ by $(Dz)^w_{xy}$ or $\overline{(Dz)}^w_{xy}$ in all expressions.

We now come to the point where we need to separate the quantum gluon field $a_\mu$ from the vacuum background field $B_\mu$, so that $A_\mu = B_\mu + a_\mu$, both satisfying periodic boundary conditions,

$$B_\mu(z_4, \boldsymbol{z}) = B_\mu(z_4 + n\beta, \boldsymbol{z}), \quad a_\mu(z_4, \boldsymbol{z}) = a_\mu(z_4 + n\beta, \boldsymbol{z}), \quad (49)$$

where $n$ is an integer. The partition function can be written as

$$Z(V,T)=\langle Z(B)\rangle_B, \quad Z(B)=N\int D\{\phi\}\exp\left(-\int_0^\beta d\tau\int d^3xL_{\rm tot}(x,\tau)\right) \tag{50}$$

where $N$ is a normalization constant and $\phi$ denotes the entire set of fields $a_\mu$, $\Psi$, $\Psi^+$. The explicit form of the Lagrangian $L_{\rm tot}$ is given in [12]. Furthermore, in (50) $\langle\ldots\rangle_B$ stands for the averaging over the (nonperturbative) background fields $B_\mu$. For our purposes one needs not know the details of this averaging.

Integration over the ghost and gluon degrees of freedom in (50) yields the same answer as for the case of $T=0$, but now all the fields are subject to the periodic boundary conditions (49). Disregarding, for the sake of simplicity, quark and source terms in $L_{\rm tot}$, one obtains

$$\begin{aligned} Z(B)=&N'(\det W(B))^{-1/2}_{reg}[\det(-D_\mu(B)D_\mu(B+a))]_{a=\delta/\delta J}\\ &\times\left\{1+\sum_{l=1}^\infty\frac{1}{l!}S_{int}\left(a=\frac{\delta}{\delta J}\right)^l\right\}\exp\left(-\frac12 JGJ\right)_{J_\mu=D_\mu(B)F_{\mu\nu}(B)}, \end{aligned} \tag{51}$$

where the valence-gluon Green's function $G\equiv W^{-1}$ is $G_{\mu\nu}=(\tilde D^2_\lambda\cdot\hat 1+2ig\tilde F_{\mu\nu})^{-1}$. We can consider strong background fields, so that $gB_\mu$ is large (as compared to $\Lambda^2_{QCD}$), while $\alpha_s=g^2/(4\pi)$ in this strong background is small at all distances. Moreover, it was shown that $\alpha_s$ is frozen at large distances [34]. In this case (51) is a perturbative sum in powers of $g^n$, arising from the expansion in $(ga_\mu)^n$.

In what follows we shall discuss the Feynman graphs for the thermodynamic potential $F(T,\mu)$, related to $Z(B)$ via

$$F(T,\mu)=-T\ln\langle Z(B)\rangle_B. \tag{52}$$

### 3.2. *Nonperturbative dynamics of quarks and gluons in the single-line approximation*

In this chapter we come to explicit calculations of various properties of the quark-gluon plasma. It is clear that (52) contains all possible interactions, perturbative and nonperturbative, between quarks and gluons and, in particular, creation and dissociation of bound states. It is impossible to take into account all possible subsystems and interaction between them, so it is imperative to choose the strategy of approximations for the quark-gluon plasma as a deconfined state of quarks and gluons.

We assume that the whole system of $N_g$ gluons, $N_q$ quarks, and $N_{\bar q}$ antiquarks remains gauge-invariant at $T>T_c$, as it was at $T<T_c$. However, in case of deconfinement and neglecting (in the first approximation) all perturbative and nonperturbative interactions, any white system possesses the same energy, depending only on the number and type of constituents. In this case the partition function factorises into a product of one-gluon and one-quark (antiquark) contributions, and one can calculate the corresponding thermodynamic potential. This first step is called the

Single Line Approximation (SLA) and below we shall calculate the results for the gas of quarks and gluons in the strong vacuum fields using our path-integral formalism. We follow [12,35–37].

In this chapter we consider gluons and quarks in SLA. Notice that, although the interaction between quarks and gluons is switched off in this approximation, there exists a strong interaction of quarks and gluons with the nonperturbative vacuum fields. We therefore keep only the lowest order in $(ga_\mu)$ but take into account interaction with the nonperturbative background vacuum fields to all orders, using the field correlator technique. As a result one can write

$$Z_0 = e^{-F_0(T)/T} = N' \langle \exp(-F_0(B)/T) \rangle_B. \tag{53}$$

Then single-gluon and single-quark contributions to the free energy can be written in the form:

$$\begin{aligned} \frac{1}{T} F_0^{gl}(B) &= \frac{1}{2} \ln \det G^{-1} - \ln \det(-D^2(B)) = \\ &= \mathrm{Tr} \left\{ -\frac{1}{2} \int_0^\infty \xi(s) \frac{ds}{s} e^{-sG^{-1}} + \int_0^\infty \xi(s) \frac{ds}{s} e^{sD^2(B)} \right\} \end{aligned} \tag{54}$$

and

$$\frac{1}{T} F_0^q(B') = \frac{1}{2} \ln \det(m_q^2 - \hat{D}^2(B')) = -\frac{1}{2} \mathrm{Tr} \int_0^\infty \xi(s) \frac{ds}{s} e^{-sm_q^2 + s\hat{D}^2(B')}, \tag{55}$$

respectively, where $B'_\nu = B_\nu - i(\mu/g)\delta_{\nu 4}$, $\mu$ is the quark chemical potential, and $m_q$ is the current quark mass (the pole mass when next terms in $\alpha_s$ are considered). The operator $\hat{D}^2(B')$ can be presented as:

$$\hat{D}^2(B') = (D_\mu \gamma_\mu)^2 = D_\mu^2(B') - gF_{\mu\nu}\sigma_{\mu\nu} \equiv D^2 - g\sigma F. \tag{56}$$

Then, using the FFSR, one can write

$$\langle F_0^{gl}(B) \rangle_B = -T \int \frac{ds}{s} \xi(s) d^4x (Dz)^w_{xx} e^{-K} \left[ \frac{1}{2} \mathrm{Tr} \langle \tilde{\Phi}_F(x,x,s) \rangle_B - \mathrm{Tr} \langle \tilde{\Phi}(x,x) \rangle_B \right], \tag{57}$$

where taking trace implies summation over the Lorentz and colour indices and $\tilde{\Phi}_F$ is defined in (9).

Similarly, one has for the quarks:

$$\langle F_0^q(B') \rangle_B = -\frac{T}{2} \int_0^\infty \frac{ds}{s} \xi(s) d^4x \overline{(Dz)}^w_{xx} e^{-K - sm^2} \mathrm{Tr} \langle \Phi_\sigma(x,x,s) \rangle_B, \tag{58}$$

where Tr implies summation over the spin and colour indices and the operator $\Phi_\sigma$ is given in (5).

For future convenience let us define the proper-time gluon and quark kernels,

$$G(s) \equiv \int (Dz)^w e^{-K} \mathrm{Tr} \langle W_\Sigma(C,s) \rangle, \quad S(s) \equiv \int \overline{(Dz)}^w e^{-K} \mathrm{Tr} \langle W_\sigma(C,s) \rangle \tag{59}$$

where

$$W_\Sigma = \frac{1}{(N_c^2 - 1)} \left[ \frac{1}{2} \tilde{\Phi}_F - \tilde{\Phi} \right], \quad W_\sigma = \frac{1}{N_c} \Phi_\sigma. \tag{60}$$

Then, using the relation between the pressure and the free energy, $PV_3 = -\langle F_0(B)\rangle_B$, one can find (the $T$-independent term with $n=0$ is subtracted, $V_3$ is set equal to unity)

$$P_{gl} = (N_c^2-1)\int_0^\infty \frac{ds}{s}\sum_{n\neq 0} G^{(n)}(s) \tag{61}$$

for gluons and

$$P_q = 2N_c\int_0^\infty \frac{ds}{s}e^{-m_q^2 s}\sum_{n=1}^{\infty}(-1)^{n+1}[S^{(n)}(s)+S^{(-n)}(s)], \tag{62}$$

for quarks, respectively.

Therefore, in order to calculate $G^{(n)}(s)$ and $S^{(n)}(s)$, one needs to evaluate the Wilson loop operators $\langle W_{\Sigma,\sigma}(C_n)\rangle$. First, we neglect the spin-dependent terms in these Wilson loops since spin-dependent interactions at $T=0$ were considered before, while their generalisation for $T>0$ is straightforward. Thus we deal with the operator $\langle W(C)\rangle$. Let us look more carefully into the topology of this Wilson loop. It is important to bear in mind that the basis states $|k\rangle$ with the quark-gluon numbers $N_g^{(k)}$, $N_q^{(k)}$, $N_{\bar q}^{(k)}$ entering the partition function,

$$Z = \sum_n \langle n|e^{-H/T}|n\rangle, \tag{63}$$

are gauge-invariant, and one can use a generic decomposition of the type: $|k\rangle = |(gg)(gg)(ggg)(q\bar q)\ldots\rangle$, where particles in parentheses form white combinations. Then, neglecting interactions between white subsystems, one finds that the contribution of such white subsystems, for example, $(gg)$ and $(q\bar q)$, to be

$$Z_{(12)} = \int d\Gamma_1 d\Gamma_2 \langle \mathrm{Tr} W(C_n^{(1)}, C_n^{(2)})\rangle, \quad d\Gamma_i = ds_i Dz_i e^{-K_i},$$

where $W(C_n^{(1)}C_n^{(2)})$ is a closed Wilson loop made of paths of the two gluons, of the $q\bar q$ pair, and, finally, of the parallel transporters (Schwinger lines) in the initial and final states — the latter are necessary to make the states gauge-invariant.

To proceed we apply the non-Abelian Stokes theorem and the Gaussian approximation (see [15,16] for the discussion and relevant references) to arrive at (15), and it is important now to specify the surface $S_n$ with the surface elements $ds_{\mu\nu}(u)$ in the integral on the r.h.s. of (15). For this analysis let us to consider colour-electric and colour-magnetic contributions separately. For the field correlator we use formulae (18).

Consider first the colour-electric piece with $\nu=\sigma=4$ (note that, by definition, $\mu<\nu$ and $\lambda<\rho$):

$$J_n^E \equiv \frac{1}{2}\int D_{i4k4}(u-v)d\sigma_{i4}(u)d\sigma_{k4}(v). \tag{64}$$

The surface $S_n$ is inside the winding Wilson loop for the gauge-invariant $q\bar q$ system. Since the correlator $D^E(u)$ vanishes at $T>T_c$, while the contribution of the correlator $D_1^E$ leads, at large interquark distances, to a sum of terms for the quarks and antiquarks separately (we shall study the interaction of quarks in chapter 4 below). Then for a single quark one obtains in this way

$$J_n^E = \frac{1}{2}\int_0^{n\beta} du_4 \int_0^{n\beta} dv_4 \int_0^{\infty} \xi d\xi D_1^E(\sqrt{(u_4-v_4)^2+\xi^2}) =$$

$$= \frac{1}{2} n\beta \int_0^{n\beta} d\nu \left(1-\frac{\nu}{n\beta}\right) \int_0^{\infty} \xi d\xi D_1^E(\sqrt{\nu^2+\xi^2}). \tag{65}$$

Note that, for $n=1$, one recovers the expression for the Polyakov loop obtained in [35,37], namely

$$L_{\rm fund} = \exp\left(-\frac{1}{2T}V_1(\infty)\right), \quad \frac{1}{2T}V_1(\infty) = J_1^E. \tag{66}$$

At this point an important simplification occurs. Originally the path $C_n$ is given by a complicated function $z_\mu(\tau)$ in four dimensions. However the integral over $d\xi$ in (65) is always from a point $z_\mu(\tau)$ on $C_n$ to infinity and it does not depend on the particular form of $C_n$ — it is the same as for the straight-line Polyakov loop. This is true, however, only for the $D_{i4k4}$ and not for $D_{iklm}$.

Another important observation is that the correlator $D_{\mu\nu\lambda\rho}(u-v)$ is not a periodic function of $(u_4-v_4)$, in contrast to the fields $F_{\mu\nu}(u)$ and $F_{\lambda\sigma}(v)$. This will be true also for the path integrals from any given point $x$ to an arbitrary point $y$, and is a consequence of the vacuum average of the parallel transporter $\Phi(u,v)$ present in $D_{\mu\nu\lambda\rho}(u-v)$.

Notice that the mixed contributions in (64),

$$J_n^{EH} \equiv \frac{1}{2}\int D_{i4kl}(u-v) d\sigma_{i4}(u) d\sigma_{kl}(v), \tag{67}$$

is $T$-independent, so we shall neglect it in what follows.

We finally turn to the spatial term, which will play a special role in what follows. Here the main contribution comes from the colour-magnetic correlator $D^H(u-v)$, which provides the area law for the (closed) spatial projection $A_3$ of the surface $S_n$. Correspondingly we shall write this term as (for $A_3 \gg T_g^2$, where $T_g$ is the gluon correlation length, $D^H(x) \sim \exp(-x/T_g)$):

$$\langle W_3(C_n)\rangle = \exp(-\sigma_s A_3), \tag{68}$$

where the spatial string tension is defined in (1) and $A_3$ is the minimal area of the spacial projection of the surface $S_n$. Similarly to the case of the $J_n^E$, one should start with white states of $q\bar{q}$, $gg$ or $3q$. As will be seen, the colour-magnetic vacuum ($D^H$) acts in the centre-of-mass frame only in the states of the system with $L \neq 0$ and the resulting contribution of the $D^H$ does not separate into single-line terms, but it rather acts pairwise (triple-wise for $3q$). Therefore one can account for colour-magnetic interaction in the higher (2-line or 3-line) terms. We shall neglect colour-magnetic interaction in the first approximation, as it is weak as compared to the colour-electric one. As a result, the 4D dynamics in (59) separates into 3D and 1D ones, and it is possible to write

$$G^{(n)}(s) \equiv G_4^{(n)}(s) G_3(s) = \int (Dz_4)^w e^{-K_4 - J_n^E} G_3(s) \tag{69}$$

and, similarly, $S^{(n)}(s) = S_4^{(n)}(s) S_3(s)$, with the free quark (gluon) factors

$$S_3^{(0)}(s) = G_3^{(0)}(s) = \int (D^3 z) e^{-K_3} = \frac{1}{(4\pi s)^{3/2}}. \tag{70}$$

One should notice at this point that $G^{(n)}(s)$ and $S^{(n)}(s)$ differ in the spin factors and in the colour group representation. Neglecting, in the lowest approximation, the spin factors, one obtains $S^{(n)}$ from $G^{(n)}$ by simply replacing adjoint quantities by fundamental ones. Note that one can use Casimir scaling [16,38] to write $\sigma_s(\mathrm{adj}) = \frac{9}{4}\sigma_s(\mathrm{fund})$.

To compute $G_4^{(n)}(s)$ one can take into account that $J_n^E$ does not depend on $z_4$ and can be pulled out of the integral, while the remaining integral over $z_4$ can be taken exactly. In particular, splitting the proper-time interval $N\varepsilon = s$, $N \to \infty$ one can write:

$$\int (Dz_4)^w e^{-K_4} = \prod_{k=1}^{N} \left( \frac{d\Delta z_4(k)}{\sqrt{4\pi\varepsilon}} e^{-\frac{(\Delta z_4(k))^2}{4\varepsilon}} e^{ip_4 \Delta z_4(k)} \right) e^{-ip_4 n\beta} \frac{dp_4}{2\pi} =$$

$$= \int \frac{dp_4}{2\pi} e^{-ip_4 n\beta - p_4^2 s} = \frac{1}{2\sqrt{\pi s}} e^{-\frac{n^2\beta^2}{4s}}. \tag{71}$$

As a result, one arrives at

$$G^{(n)}(s) = \frac{1}{2\sqrt{\pi s}} e^{-\frac{n^2\beta^2}{4s} - \tilde{J}_n^E} G_3^{(0)}(s) \tag{72}$$

$$S^{(n)}(s) = \frac{1}{2\sqrt{\pi s}} e^{-\frac{n^2\beta^2}{4s} - J_n^E} S_3^{(0)}(s), \quad \tilde{J}_n^E = \frac{9}{4} J_n^E.$$

Substituting (69) – (72) into (61) and (62), one arrives at the expressions for the pressure with the only unknown quantity being the fundamental Polyakov line $J_n^E$. In the next chapter we discuss in detail the behaviour of the Polyakov lines at finite temperatures.

### 3.3. *Polyakov lines at finite temperatures*

An important result of the previous chapter is that colour-electric correlator $D_1^E$ yields factorised contribution, that is $Z_{(12)} = Z_1 Z_2$, where each individual factor $Z_i$ contains only the part of the common loop in the form of the Polyakov loop factor (with the singlet free energy in the exponent). The contribution of colour-magnetic fields does not factorize, however, this contribution can be considered as a correction, so it will be neglected. In addition, the average of the Polyakov line operator was related to the colour-electric correlator $J_1^E$ and to the static potential $V_1(\infty)$. In this chapter we discuss the behaviour of the Polyakov lines and static potentials in the Gaussian approximation to the QCD vacuum.

At $T_c > T > 0$ one has four Gaussian correlators $D^E(x)$, $D_1^E(x)$, $D^H(x)$, and $D_1^H(x)$, with the string tensions $\sigma^{E,H}$ given by (1). At $T > T_c$ the correlator $D^E$ (and, consequently, $\sigma^E$) vanishes, as was suggested in [9,11] and then was proved on the lattice [8]. The three remaining correlators are nonzero, moreover the spatial string tension $\sigma_s \equiv \sigma^H$ grows with the temperature in the dimensionally reduced limit [39]. This fact explains also the growth with temperature of the Debye mass, $m_D \cong 2\sqrt{\sigma_s}$ [40,41], which is known from the lattice data [33]. Apart from this quantity, we shall not use below, in this section, the colour-magnetic correlators, since they do not produce static potentials between particles in the relative $S$-wave. Therefore we are interested only in the colour-electric correlators $D^E(x)$ (inside the confined phase bounded by the curve $T_c(\mu)$) and $D_1^E(x)$ (in the whole $\mu, T$ plane).

Let us stress once more that, in our approach, only gauge-invariant states $|n\rangle$ are to be considered in the partition function (63) at $T > 0$. This is evident in the confined phase, since any coloured part of the given gauge-invariant system is connected to other parts by strings. In absence of colour-electric strings in the deconfined phase the necessity of using gauge-invariant amplitudes is less evident, except for world-lines in the spatial directions, where colour-magnetic confinement with a nonzero $\sigma_s$ is operating. Our use of gauge-invariant amplitudes, which factorise at large interparticle distances in the deconfined phase, leads to an explicit prediction for the EoS with modulus of phase factors, which approximately equal to modulus of Polyakov lines.

Below we use, as in [35,36], gauge-invariant states, $|n\rangle$ at all temperatures and chemical potentials and describe the interparticle dynamics in terms of gauge-invariant quantities, like pair-wise or triple static potentials. The large-distance limit of these potentials yields one-particle characteristics — the self-energy parts of quarks, antiquarks, gluons, and so on. One can use those to study thermodynamics of QGP in the one-particle, or SLA [35,36]. It is rewarding, that the field correlator method is a natural instrument in describing this deconfined dynamics since, in absence of the $D^E$, the correlator $D_1^E$ has the form of the full derivative and produces gauge-invariant one-particle pieces — self-energy parts — automatically (in addition to the interparticle interaction decreasing at large distances).

Gauge-invariant states $|n\rangle$, formed with the help of parallel transporters (Schwinger lines) (4), create, as shown in [35], Wilson loops $W(C)$ for $q\bar{q}$, $qqq$, or other quark systems. Lattice data allow one to extract static interquark potentials in such multiquark systems [42,43]. When treating coloured systems, like $(qq)$, taken as a part of a gauge-invariant system ($qq\bar{q}\bar{q}$ in this case), the pairs $(qq)$ and $(\bar{q}\bar{q})$ are separated at a large distance and the potential $V(qq, \bar{q}\bar{q})$ is neglected.

We start from the colour-singlet $q\bar{q}$ system and write contributions of the $D^E$, and $D_1^E$ to the static potentials at a nonzero $T = 1/\beta$ [42]:

$$V_0(r,T) = 2\int_0^\beta d\nu(1-\nu T)\int_0^r (r-\xi)d\xi D^E(\sqrt{\xi^2+\nu^2}), \tag{73}$$

$$V_1(r,T) = \int_0^\beta d\nu(1-\nu T)\int_0^r \xi d\xi D_1^E(\sqrt{\xi^2+\nu^2}), \tag{74}$$

which contribute to the modulus of the Polyakov loops as

$$L^{(V)}_{\rm fund} = \exp\left(-\frac{V_1(T)+2V_0}{2T}\right), \quad L^{(V)}_{\rm adj} = \left(L^{(V)}_{\rm fund}\right)^{9/4} \tag{75}$$

where $V_1(T) \equiv V_1(\infty,T)$, $V_0 \equiv V_0(r^*,T)$, and $r^*$ is an average distance between the heavy-quark line and light antiquark (for $n_f > 0$) or between the "heavy-gluon line" and a gluon for $L_{\rm adj}$. The Casimir scaling relation (75) predicted in [16] is in good agreement with lattice data [33], as well as vanishing of the $L_{\rm fund}$ for $T \le T_c$, $n_f = 0$ and the strong decrease of $L_{\rm adj}$ for $T \le T_c$. Indeed, for $T \le T_c$ and $n_f = 0$ one has $r^* \to \infty$ and $V_0 \to \infty$, explaining vanishing of the $L^{(V)}_{\rm fund}$. For the $L^{(V)}_{\rm adj}$ in this region one can take into account the kinetic energy of the gluon in the system consisting of an adjoint source plus a gluon (gluelump). This yields an estimate $L_{\rm adj}(T \le T_c) = \exp(-m_{glp}/T)$, where $m_{glp}$ was computed in [41] to be of order 1 GeV.

Notice that the Polyakov lines measured on the lattice are expressed through the (singlet) free energy of a $Q\bar Q$ system at large distances $F^1_{Q\bar Q}(\infty,T)$, in the same way as in (75),

$$L^{(F)}_{\rm fund} = \exp\left(-\frac{F^1_{Q\bar Q}(\infty,T)}{2T}\right). \tag{76}$$

In order to relate $L^{(F)}_j$ and $L^{(V)}_j$ one can use the standard representation for the free energy $F^1_{Q\bar Q}(r,T)$,

$$\exp\left(-\frac{F^1_{Q\bar Q}(r,T)}{T}\right) = \sum_{n(Q\bar Q)} c_n \exp\left(-\frac{V_n^{Q\bar Q}(r,T)}{T}\right), \tag{77}$$

where the summation covers all excited and bound states involving $Q\bar Q$, and $V_n^{Q\bar Q}(r,T)$ is the energy term of such a state $n$ with the distance between the static charges $Q$ and $\bar Q$ being equal to $r$. It is clear that $L^{(V)}_j$ coincides with $L^{(F)}_J$ when all states $n$, except for the ground state $n=0$, are neglected. In this case $V_0^{Q\bar Q}(r,T)$ coincides with $V_1(r,T)$ and, hence, with the $F^1_{Q\bar Q}(r,T)$. Note that $V_1(r,T)$ in (74) does not depend on $T$ in the string limit of QCD, when the vacuum correlation length $T_g$ tends to zero.

In the general case all states $n(Q\bar Q)$ contribute and therefore ($c_n > 0$) one has the following inequality:

$$V_1(r,T) \ge F^1_{Q\bar Q}(r,T) \tag{78}$$

In order to define $V_1$ and $L_{\rm fund}$ properly one needs to separate their perturbative and nonperturbative parts and to renormalise $V_1$ to get rid of perimeter divergences. The separation in $D_1^E(x)$ can be seen at small $x$ [44]

$$D_1^E(x)=\frac{4C_F\alpha_s}{\pi}\left[\frac{1+O(\alpha_s\ln^k x)}{x^4}+\frac{\pi^2G_2}{24N_c}+\dots\right]=\left(D_1^E\right)^{\rm pert}+\left(D_1^E\right)^{\rm np}, \quad (79)$$

and at large $x$, where $\left(D_1^E\right)^{\rm np}(x)$ behaves as [44]:

$$\left(D_1^E\right)^{\rm np}(x)\cong A_1\frac{e^{-M_0|x|}}{|x|}, \quad A_1=2C_F\alpha_sM_0\sigma_{\rm adj}, \quad (80)$$

where $M_0$ is the lowest gluelump mass [41], $M_0\approx 1$ GeV, $C_F=(N_C^2-1)/(2N_C)=4/3$ is the fundamental Casimir operator, and $G_2$ is the gluon condensate, $G_2=(\alpha_s/\pi)\langle F^a_{\mu\nu}F^a_{\mu\nu}\rangle$.

The corresponding separation of the $V_1(r,T)$ is done in [42] and reads:

$$V_1(r,T)=V_1^{\rm pert}(r,T)+V_1^{\rm np}(r,T)+V_1^{\rm div}(a), \quad (81)$$

where

$$V_1^{\rm pert}(r,T)=-\frac{C_F\alpha_s}{r}e^{-m_Dr}(1+O(rT)), \quad (82)$$

$V_1^{\rm np}$ is given by (74), with the substitution $D_1^E\to(D_1^E)^{\rm np}$, and

$$V_1^{\rm div}(a)\cong\frac{2C_F\alpha_s}{\pi}\left(\frac{1}{a}+O(T\ln a)\right). \quad (83)$$

Here $m_D=m_D(T)\approx 2\sqrt{\sigma_s}$ is the nonperturbative Debye mass [40] and $a$ is the lattice spacing (cut-off).

The renormalisation procedure suggested in [42] amounts to discarding $V_1^{\rm div}(a)$, and this is in agreement with the lattice renormalisation used in [43], where $F^1_{Q\bar Q}(r,T)$ was adjusted to the form $V_1^{\rm pert}(r,T)$ at small $r$ and $T$. Note, that $V_1^{\rm np}(r,T)\sim O(r^2)$ in this region and the procedure indeed allows one to eliminate the constant term $V_1^{\rm div}(a)$.

Let us discuss now the contribution of the $V_1$ to the interaction in $Q\bar Q$, $QQ$, and $3Q$ systems. We start with the one-particle limit of the $V_1(r,T)$ and the corresponding contribution to the $L^{(V)}_{\rm fund}$. According to the discussion above, one defines the renormalised Polyakov loop as in (75), (81), with $V_1(T)\equiv V_1^{\rm np}(\infty,T)$. We shall neglect the difference between $L_j^{(V)}$ and $L_j^{(F)}$ (this difference becomes important at large $T$'s, when $L^{(F)}_{\rm fund}>1$, while $L^{(V)}_{\rm fund}<1$).

From (80) one has (at $T\le T_c$):

$$V_1^{\rm np}(\infty,T)=\frac{A_1}{M_0^2}\left[1-\frac{T}{M_0}\left(1-e^{-\frac{M_0}{T}}\right)\right], \quad (84)$$

so that, for $M_0\approx 1$ GeV,

$$V_1^{\rm np}(\infty,T_c)\approx\frac{6\alpha_s(M_0)\sigma_{\rm f}}{M_0}\approx 0.5 \text{ GeV}. \quad (85)$$

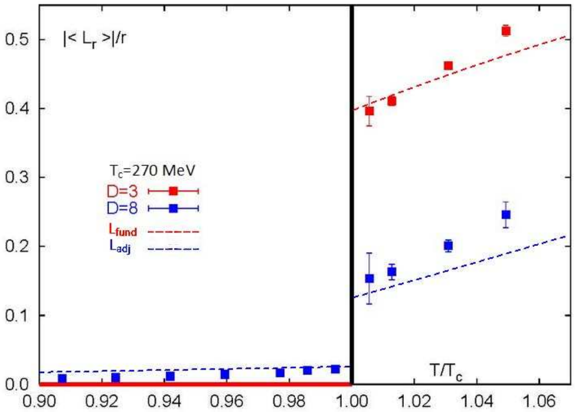

Fig. 1. Shown on the figure are curves of $L_{\rm adj}$ (blue dashed) and $L_{\rm fund}$ (red dashed) compared to the ones taken from [33]. In the $T < T_c$ region the $M(\bar{\alpha}_s = 0.195) = 0.982$ GeV gluelump mass was used. In the deconfinement region the fit (86) was used with $T_c = 270$ MeV for $L_{\rm fund}$ and the Casimir scaled value for $L_{\rm adj}$.

A similar estimate one obtains from the lattice data [45] which, at $T \sim T_c$, can be parameterize as

$$F^1_{Q\bar{Q}}(\infty, T) \approx \frac{0.175}{1.35\left(\frac{T}{T_c}\right) - 1}, \quad F^1_{Q\bar{Q}}(\infty, T_c) \approx 0.5 \text{ GeV}. \tag{86}$$

Thus quarks (and antiquarks) have self-energy parts which, at $T \approx T_c$, are given by $\kappa_q(T) = \kappa_{\bar{q}}(T) = V_1(T)/2 \approx F^1_{Q\bar{Q}}(\infty, T)/2 \approx 0.25$ GeV.

To illustrate the discussion of the $V_0$, $V_1$, and $L_{\rm fund}$, $L_{\rm adj}$ we compare in Fig. 1 our theoretical curves for the $L_{\rm fund}$ and $L_{\rm adj}$ (dashed curves) with the lattice data taken from [33] (dots). The theoretical curves follow from (75), with $V_1(\infty, T) = F^1_{Q\bar{Q}}(\infty, T)$ taken from (86) for $T > T_c$ and $L_{\rm adj} = \exp\left(-\frac{M_0}{T}\right)$ for $T \leq T_c$. From Fig. 1 one can see a good agreement between our theoretical predictions and the lattice data.

Similarly, for gluons, one has at $T \sim T_c$ that $\kappa_g(T) = (9/4)\kappa_q(T) \approx 0.56$ GeV.

Let us turn now to the $r$-dependence of the interaction. The perturbative part has a standard screened Coulomb behaviour (82), while the nonperturbative part vanishes at small $r$'s:

$$V_1^{\rm np}(r, T) \underset{r \to 0}{\sim} {\rm const} \cdot r^2. \tag{87}$$

From (74) and (80) one has [42]

$$V_1^{\rm np}(r, T) = V_1^{\rm np}(\infty, T) - \frac{A_1}{M_0^2} K_1(M_0 r) M_0 r + O\left(\frac{T}{M_0}\right) \equiv V_1^{\rm np}(\infty, T) + v(r, T). \tag{88}$$

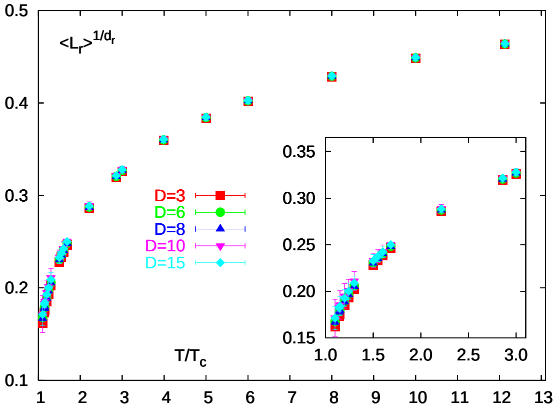

Fig. 2. The Casimir-scaled bare Polyakov loops for different representations $D$ measured on $32^3 \times 4$ lattices [33].

Therefore the nonperturbative interaction in the white system $Q\bar{Q}$ changes from $V_1^{\rm np}(\infty,T) \approx 0.5$ GeV at large $r$'s to zero at small $r$'s. The same (multiplied by the factor 9/4) is true for the white $gg$ system.

We conclude this chapter by a discussion of the role of excited states in the definition of the $F^1_{Q\bar{Q}}$ and of a possible violation of the Casimir scaling for the $L_{\rm fund}$ and $L_{\rm adj}$. It is clear that in the $F^1_{Q\bar{Q}}$ for $n_f = 0$ the only possible excited states consist of gluons: $(Qg)(\bar{Q}g)$, $(Qgg)(\bar{Q}gg)$, and so on. As it was shown in [46], the weakly bound states $(Qg)$ are indeed supported by $V_1(r,T)$ and, in neglect of the small binding energy, the total energy of these states is roughly given by the sum of the self-energy parts $\kappa_Q$ and $\kappa_g$,

$$E_{Qg} \approx \frac{1}{2}V_1(\infty,T) + \frac{9}{8}V_1(\infty,T) \approx 0.8 \text{ GeV}(T \approx T_c). \tag{89}$$

This should be compared with the possible bound state of an adjoint static source $G$ plus gluon which, in the weakly binding limit, can be written as

$$E_{Gg} \approx 2 \times \frac{9}{8}V_1(\infty,T) \approx 1.1 \text{ GeV}(T \approx T_c). \tag{90}$$

Notice that multiplicities of the states (89) and (90) are different, which leads to different predictions for corrections to the $F^1_{Q\bar{Q}}$ and $F^1_{GG}$. These corrections are not connected by the Casimir scaling, in contrast to the main (ground-state) term, for which $V^1_{Q\bar{Q}} = V_1(\infty,T)$ and $V^1_{GG} = \frac{9}{4}V_1(\infty,T)$. Therefore one expects some violation of the Casimir scaling by gluon-induced bound states in the $L_{\rm fund}$ and $L_{\rm adj}$, though high precision lattice data [33] indicate a small role of such bound states.

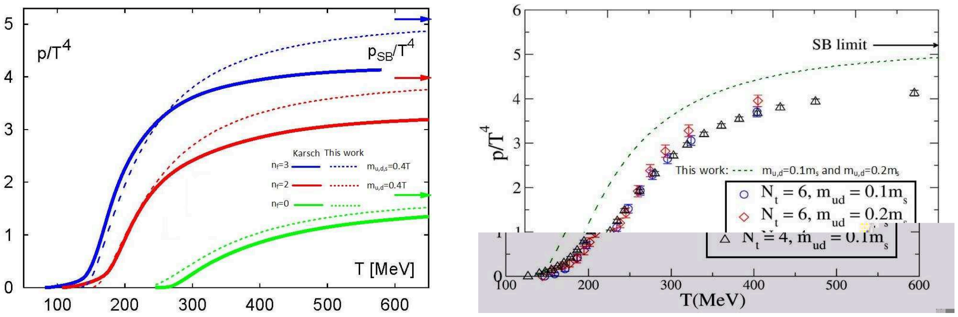

Fig. 3. Pressure $\frac{P}{T^4}$ as function of temperature $T$. Shown on the left figure is a comparison of the analytical calculus (95)(dashed lines) with the lattice results (bold lines) [47] for the case $n_f = 0, 2, 3$. Shown on the right figure is the case of $n_f = 2+1$. Green dashed line is the analytical calculation (94) compared to the lattice one from [48].

### 3.4. *Equation of state*

Here we follow the approach to study the QGP dynamics [35,36], where the main emphasis was done on the vacuum fields, and the resulting modification of quark and gluon propagators was considered as the first and the basic step in the nonperturbative treatment of QGP — the SLA discussed before. As a result one obtains the nonperturbative EoS of QGP in the form of free quark and gluon terms multiplied by the vacuum induced factors. The latter are expressed via the only (nonconfining) colour-electric correlator $D_1^E(x)$ and happened to be approximately equal to the absolute values of Polyakov loops $L_{\rm fund}$, $L_{\rm adj}$ for quarks and gluons, respectively. Furthermore, due to the Casimir scaling property [33,16], these Polyakov loops are related to one another, as $L_{\rm adj} = (L_{\rm fund})^{9/4}$.

Moreover, the phase diagram was calculated in the SLA assuming that the phase transition is vacuum dominated, that is, a transition from the confining vacuum with vacuum energy density $\varepsilon_{\rm conf} \cong -\frac{\beta_0}{32} G_2({\rm conf})$ to the nonconfining vacuum with $\varepsilon_{\rm dec} \cong -\frac{\beta_0}{32} G_2({\rm dec})$. The resulting phase curve $T_c(\mu)$ in [49] depends on $\Delta G_2 = G_2({\rm conf}) - G_2({\rm dec})$ and it was found to be in good agreement with lattice data [50] for standard values of the $G_2({\rm conf})$ and $\Delta G_2 \approx 0.5 G_2$ — this will be discussed in detail in the next chapter.

Thus the SLA is a reasonable starting point with no fitting or model parameters, since $L_{\rm fund}$ can be computed analytically [44] or on the lattice [33], and $\Delta G_2 \approx 0.5 G_2$ is a fundamental parameter of QCD. This picture of the QCD phase transition was called in [49] the Vacuum Dominance Model (VDM) originally proposed in [9,10] in a simplified form (sometimes called the Evaporation Model).

In this chapter we exploit the reduced pressure $p = \frac{P}{T^4}$, and combine (61),(62)

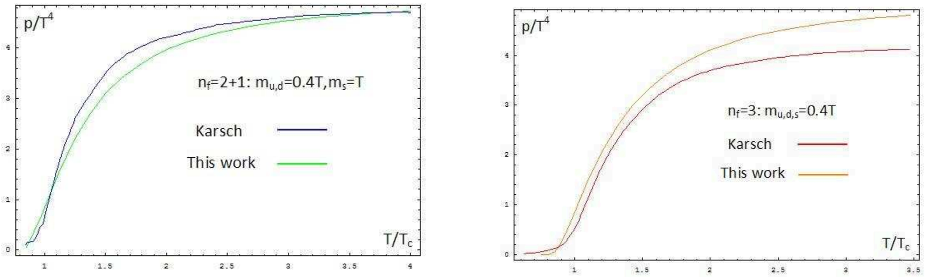

Fig. 4. Pressure $\frac{P}{T^4}$ as function of temperature $T$. The case of $n_f = 2+1$ (left figure) and $n_f = 3$ (right figure) (95). Lattice results were taken from [50].

and (71),(72) to obtain a simple form, which can be written as:

$$p_q = \frac{P_q^{SLA}}{T^4} = \frac{4N_c n_f}{\pi^2} \sum_{n=1}^{\infty} \frac{(-1)^{n+1}}{n^4} L^n_{\rm fund} \varphi_q^{(n)} \tag{91}$$

and

$$p_{gl} = \frac{P_{gl}^{SLA}}{T^4} = \frac{2(N_c^2-1)}{\pi^2} \sum_{n=1}^{\infty} \frac{1}{n^4} L^n_{\rm adj}, \tag{92}$$

for quarks and gluons, respectively. Here $\varphi_q^{(n)}$ is

$$\varphi_q^{(n)} = \frac{n^2 m_q^2}{2T^2} K_2\left(\frac{n m_q}{T}\right) = \frac{n^4}{6} \int_0^\infty \frac{z^4}{\sqrt{z^2+\nu^2}} e^{-n\sqrt{z^2+\nu^2}} dz, \quad \nu = \frac{m_q}{T}, \tag{93}$$

where an integral representation of the Bessel function $K_2$ was used in the second equality. Then both sums (91) and (92) can be evaluated explicitly to yield:

$$p_q = \frac{2N_c}{3} \frac{n_f}{\pi^2} \int_0^\infty \frac{z^4}{\sqrt{z^2+\nu^2}} \frac{dz}{e^{\sqrt{z^2+\nu^2}+a}+1}, \quad p_{gl} = \frac{N_c^2-1}{3\pi^2} \int_0^\infty \frac{z^3 dz}{e^{z+a_{gl}}-1}, \tag{94}$$

with $a_q = V_1(T)/2T$, $a_{gl} = \frac{9}{4} a_q$.

Here we consider the case of $\mu = 0$ (generalisation to the case of nonzero chemical potentials will be discussed in chapter 5) and characteristic temperature region of $T \approx T_c$ ($T_c = 170 \div 270$ MeV) where quark masses do not affect the thermodynamical functions appreciably. This is due to the fast convergence of the sum over $n$ at large $n$'s ensured by the factors $1/n^4$ and $L^n$ ($L < 1$), while $\varphi_q^{(n)} \approx 1$ for $n \simeq 1$. Indeed, for $m_q = 0$ $\varphi_q^{(n)} = 1$, whereas for $m_q = 0.4T$ one has $\varphi_q^{(1)} = 0.96$, while $\varphi_q^{(15)} = 0.03$. Therefore one can neglect, with a good accuracy, the masses in (94), arriving at:

$$p_q = \frac{2n_f}{\pi^2} \int_0^\infty \frac{z^3 dz}{e^{z+a_q}+1}, \quad p_{gl} = \frac{8}{3\pi^2} \int_0^\infty \frac{z^3 dz}{e^{z+a_{gl}}-1}. \tag{95}$$

The results presented in (95) are compared with the lattice pressure data, in Figs. 3, for $n_f = 2+1$ (left) and $n_f = 3$ (right figure). In Fig. 4 we show our

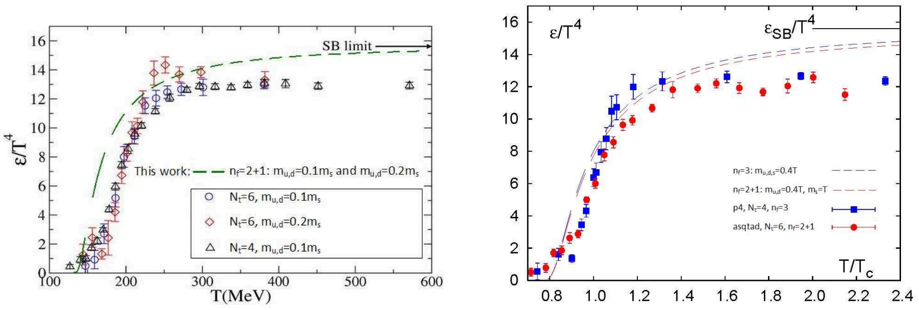

Fig. 5. Energy density $\frac{\varepsilon}{T^4}$ as function of temperature $T$. The case $n_f = 2+1$ with $m_{u,d} = 0.1m_s$ and $m_{u,d} = 0.2m_s$ (green dashed curve) (97) is compared to lattice data from [48](left fig.). The case $n_f = 2+1$ with $m_{u,d} = 0.4T$, $m_s = T$ (red dashed curve) and $n_f = 3$ with $m_q = 0.4T$ (blue dashed curve) (97) are compared to lattice data from [47](right fig.).

calculated curves for the cases $n_f = 2+1$ (left part) and $n_f = 3$ (right part), which are compared with lattice data from [50].

As a further simplification, one can use, instead of (95), the first terms of the expansion in (91), (92), namely:

$$p_q = \frac{12n_f}{\pi^2} L_{\rm fund}, \quad p_g = \frac{16}{\pi^2} L_{\rm adj}. \tag{96}$$

Other useful quantities to compare with the lattice data are the internal energy density and the "nonideality" of the QGP:

$$\varepsilon = T^2 \frac{\partial}{\partial T} \left( \frac{P}{T} \right)_V = \varepsilon_q + \varepsilon_{gl} \tag{97}$$

and

$$I(T) = \frac{\varepsilon - 3P}{T^4} = T \frac{\partial p}{\partial T}, \tag{98}$$

respectively.

Using (94) and (96) one has

$$\varepsilon_q^{(0)} = \sum_{n_f} \frac{2}{\pi^2} T^2 \frac{d}{dT} \left( T^3 \int_0^\infty \frac{z^4}{\sqrt{z^2+\nu^2}} \frac{dz}{e^{\sqrt{z^2+\nu^2}+a_q}+1} \right), \tag{99}$$

$$\varepsilon_{gl}^{(0)} = \frac{3}{3\pi^2} T^2 \frac{d}{dT} \left( T^3 \int_0^\infty \frac{z^3 dz}{e^{z+a_{gl}}+1} \right), \tag{100}$$

and

$$I(T) = \frac{12n_f}{\pi^2} T \frac{dL_{\rm fund}}{dT} + \frac{16}{\pi^2} T \frac{dL_{\rm adj}}{dT} \tag{101}$$

The results of the calculations for $\frac{\varepsilon}{T^4}$ are compared, in Fig. 5, 6, with three different sets of the lattice data: [47],[48], and [51]. In Fig. 7 we demonstrate the $I(T)$,

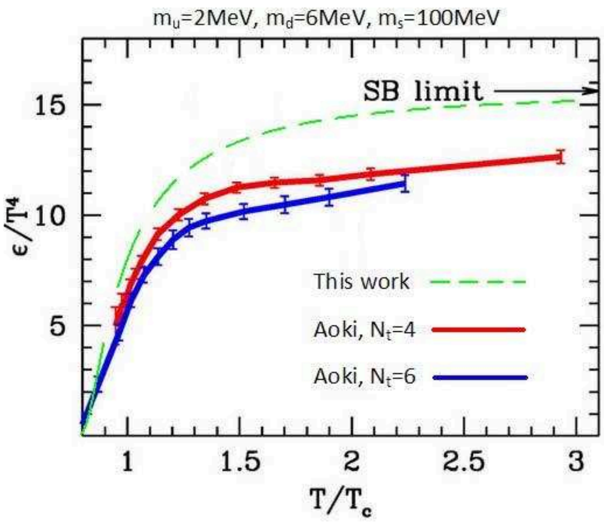

Fig. 6. Energy density $\frac{\varepsilon}{T^4}$ as function of temperature $T$. The curve for $n_f = 3$ with $m_u = 2$ MeV, $m_d = 6$ MeV, $m_s = 100$ MeV (green dashed) (97) is compared to lattice data from [51].

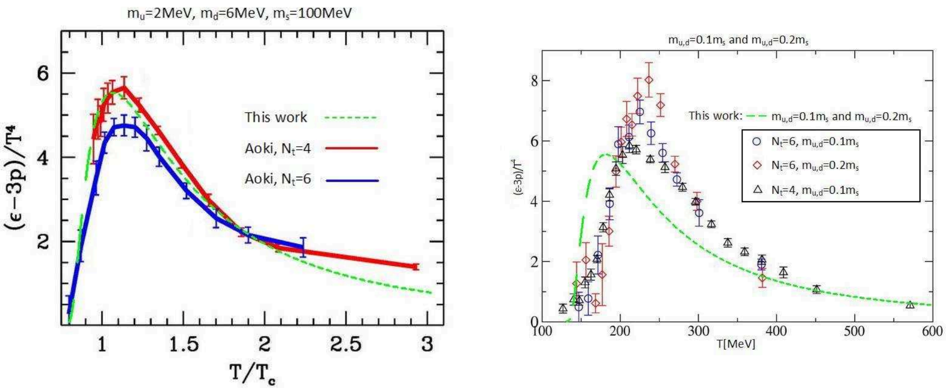

Fig. 7. "Nonideality" of QGP $(\varepsilon - 3p)/T^4$. Shown are the curves for (left fig.) $n_f = 3$ with $m_u = 2$ MeV, $m_d = 6$ MeV, $m_s = 100$ MeV (green dashed line) compared to [51] and (right fig.) for $n_f = 2 + 1$ with $m_{u,d} = 0.1 m_s$ and $m_{u,d} = 0.2 m_s$ compared to [48]. Analytical calculations are done using (94) and (97).

computed with the help of (101) and (95), with lattice data for 2+1 flavours from [51] (left curve) and from [48] (right curve).

It is instructive to estimate the contribution of the $q\bar{q}$ and $gg$ interactions to the pressure. Writing the virial coefficient in the form $P_j = P_j^{(0)}(1 + (P_j^{(0)}/T)B_j(T) +$

...), where $P_j^{(0)}=P_q$ or $P_{gl}$ in the SLA, with

$$B_j(T)=\frac{1}{2}\int\left(1-e^{U_j(r,T)/T}\right)dV,\quad j=\text{fund, adj},\tag{102}$$

and taking the interaction terms $U_{\rm fund}$ and $U_{\rm adj}$, at large $T$, as $U_j(r,T)=Tu_j(rT)$, one obtains a corrected pressure in the form:

$$P=P_q^{(0)}(1-c_q)+P_{gl}^{(0)}(1-c_{gl})\tag{103}$$

where

$$c_{gl}\cong\frac{16}{\pi^2}\int_0^\infty\rho^2d\rho(e^{|u_{\rm adj}(\rho)|}-1),\quad c_q\cong\frac{12n_f}{\pi^2}\int_0^\infty\rho^2d\rho(e^{|u_{\rm fund}(\rho)|}-1).\tag{104}$$

Note that the $q\bar{q}$ and $gg$ interactions in the singlet colour state is attractive, so that $|U_j|=-U_j$. The dependence of the $u_j$ on $rT$ occurs at large $T$ (in the dimensionally reduced regime), when the dynamical dimensional quantities are the spatial string tension $\sigma_H=\text{const}\cdot T^2$ and the Debye mass $m_D(T)\cong 2\sqrt{\sigma_H}=\text{const}\cdot T$.

Thus one expects that: i) the corrected pressure (103) is smaller than the SLA prediction and ii) the large-$T$ behaviour of the $P(T)$ is below the Stefan-Boltzmann values (modulo logarithmic factors). Both features are clearly seen in Figs. 4, 5.

## 4. Beyond Single Line Approximation: Interacting quarks and gluons

In the previous Sections one-particle contributions to the partition function were considered in the so-called SLA. It was stressed however that, at $T>T_c$, some interactions, like the residual colour-electric and colour-magnetic one, acts in white ensembles of quarks and gluons. Such interactions were neglected before, except for the contributions of the correlator $D_1^E$ which produced effectively single-line term $V_1(\infty)$. In addition, $D_1^E$ as well as $D^H$, and $D_1^H$ produce bound systems of quarks and gluons [13,42,46] which may affect strongly the dynamics of the QGP at $T\geq T_c$. Such bound states will be discussed below. To this end we start from a Green's function of the given quark(gluon) system and extract, in the same way as it was done before for the quark-antiquark meson at $T=0$, the corresponding Hamiltonian $H$,

$$G({\rm out}|{\rm in})=\langle{\rm out}|e^{-H/T}|{\rm in}\rangle.\tag{105}$$

Our purpose in this Section is to discuss the properties of this resulting Hamiltonian and possible consequences for the quark-gluon thermodynamics. Bound states in the $q\bar{q}$, $gg$, and $gq$ systems were studied in the framework of the FCM [42,46] and on the lattice — see [52] and references in [42,46]. One can consider two distinct dynamics: the colour-electric one, due to $D_1^E$, and the colour-magnetic one, due to $D^H$ and $D_1^H$.

| | $(Q\bar{Q})_1$ | $(Q\bar{Q})_8$ | $(QQ)_3$ | $(QQ)_6$ | $(Qg)_3$ | $(Qg)_6$ | $(gg)_1$ | $(gg)_8$ |
|---|---|---|---|---|---|---|---|---|
| $a$ | 0 | 9/8 | 1/2 | 5/4 | 1/2 | 5/4 | 0 | 9/8 |
| $b$ | 1 | -1/8 | 1/2 | -1/4 | 9/8 | 3/8 | 9/4 | 1 |

Table 1. Parameters of the static potential of binary systems $(Q\bar{Q})_D$, $(QQ)_D$, $(Qg)_D$, and $(gg)_D$ in different colour representations $D$.

### 4.1. *Bound states at* $T > T_c$ *due to colour-electric forces*

In the colour-electric case the interaction can be written as (see [42,46] for the discussion):

$$V^E_{q\bar{q}}(r,T) \equiv v_1(r,T) \equiv V_1(r,T) - V_1(\infty,T) \tag{106}$$

where

$$V_1(r,T) = \int_0^{1/T} (1-\nu T)d\nu \int_0^r \xi d\xi D_1^E(\sqrt{\nu^2+\xi^2}). \tag{107}$$

Notice that, in (106), we subtracted $V_1(\infty,T)$ which was already accounted in the SLA, in the form of the Polyakov lines — see (66).

Characteristic feature of $v_1(r,T)$ is that it is short-ranged, $r_{eff} \sim 0.3$ fm, and it can support bound $S$-wave states in $(c\bar{c})_1$, $(gg)_1$, $(cg)_3$, and $(gg)_8$ (the subscript stands for the representation of the colour group). The binding is weak, $|\varepsilon| \lesssim 0.14$ GeV for $T \lesssim 1.5T_c$. On the lattice, in addition to $S$-wave states $(c\bar{c})_1$, $(b\bar{b})_1$, and light $(q\bar{q})$, the lowest $P$-wave state is claimed to exist (see [52] for a review).

It is clear that weakly bound states should dissociate fast in the dense QGP and therefore they hardly produce any significant effect on the production rate. They are important, however, for the kinetic coefficients.

First, we generalise the static interaction (107) to the case, when two colour objects, $A$ and $B$, combine into a common colour state $D$ [b]

$$V_1^{(AB,D)}(r,T) = \frac{1}{2C_F}\{C_D V_1^{(Q\bar{Q})}(\infty,T) + (C_A + C_B - C_D)V_1^{(Q\bar{Q})}(r,T)\}$$

$$\equiv \bar{a}V_1^{(Q\bar{Q})}(\infty,T) + \bar{b}V_1^{(Q\bar{Q})}(r,T). \tag{108}$$

Here $C_F = \frac{4}{3}$ is the Casimir operator for the fundamental charges, while $C_A$, $C_B$, and $C_D$ are that for the representations $A$, $B$, and $D$, respectively. In Table 1 we illustrate (108).

---

[b] The construction is similar to that found in [53] for the coefficient $\bar{b}$ of the $V_1^{(Q\bar{Q})}(r,T)$ but differs in the presence of the first term proportional to $\bar{a}$, since in [53] the constant term was not taken into account.

For multicomponent systems one can similarly find,

$$V_1^{(ABC,D)}(\boldsymbol{r}_1,\boldsymbol{r}_2,\boldsymbol{r}_3,T)=\frac{1}{2C_F}\{C_DV_1^{(Q\bar{Q})}(\infty,T)$$

$$+\frac{1}{3}(C_A+C_B+C_C-C_D)\sum_{i>j}V_1^{(Q\bar{Q})}(\boldsymbol{r}_i-\boldsymbol{r}_j,T)\}. \tag{109}$$

In particular,

$$V_1^{(QQQ)}=\frac{1}{2}\sum_{i>j}V_1^{(Q\bar{Q})}(\boldsymbol{r}_i-\boldsymbol{r}_j,T) \tag{110}$$

$$V_{10}^{(QQQ)}=\frac{9}{4}V_1^{(Q\bar{Q})}(\infty,T)-\frac{1}{4}\sum_{i>j}V_1^{(Q\bar{Q})}(\boldsymbol{r}_i-\boldsymbol{r}_j,T) \tag{111}$$

$$V_8^{(QQQ)}=\frac{9}{8}V_1^{(Q\bar{Q})}(\infty,T)+\frac{1}{8}\sum_{i>j}V_1^{(Q\bar{Q})}(\boldsymbol{r}_i-\boldsymbol{r}_j,T). \tag{112}$$

It is easy to check that, at large distances, all systems consisting of $n_Q$ quarks or antiquarks and $n_g$ gluons tend to the constant limit, independent of $D$,

$$V_1^{(n_QQ,n_gg)}(|\boldsymbol{r}_i-\boldsymbol{r}_j|\to\infty)=E_Qn_Q+E_gn_g, \tag{113}$$

where

$$E_Q=\frac{1}{2}V_1^{(q\bar{Q})}(\infty,T),\quad E_g=\frac{9}{8}V_1^{(Q\bar{Q})}(\infty,T). \tag{114}$$

Since the nonperturbative part of the $V_1^{(Q\bar{Q})}(r,T)$ behaves as $O(r^2)$ at $r\to 0$, one obtains the lower bound on the nonperturbative part of $V^{(n_QQ,n_gg)}(r_{ij},T)$: $V^{(n_QQ,n_gg)}(r_{ij},T)\gtrsim(1/2)(C_D/C_F)V_1^{(Q\bar{Q})}(\infty,T)$. As a consequence, one can predict the absence of bound states in some particular channels, for example, in $(Q\bar{Q})_8$, $(QQ)_6$, $(QQQ)_{10}$, and so on.

As an application of the general relation (87) we show, in Fig. 8, the static potentials $V^{(QQQ)}(\boldsymbol{r}_1,\boldsymbol{r}_2,\boldsymbol{r}_3,T)=V^{(D)}(r,T)$ of three static fundamental quarks in three different representations $D$: singlet ($C_D=0$), octet ($C_D=3$) and decuplet, ($C_D=6$). The quarks form a symmetric configuration of a equilateral triangle with the sides $r$. From Fig. 8 one can see that, indeed, all three potentials tend to the same limit $(3/2)V_1^{(Q\bar{Q})}(r,T)$ at large $r$'s, in agreement with (113), while deviations from this asymptotic at all distances are proportional to $(1/2,-1/4,1/8)$ for the singlet, decuplet, and octet, respectively, as prescribed by (110)-(112). This is in agreement with lattice calculations of free energies $F_{qqq}^{(D)}(r,T)$ presented in [54].

Having constructed static potentials, we can now exploit the relativistic Hamiltonian technique, developed in [23,21] and successfully used for mesons, baryons, glueballs, and hybrids in the confinement phase (see [6,7] for a review). This technique does not take into account chiral degrees of freedom. Therefore, below we stick to the Hamiltonian technique of [21] and consider heavy quarkonia and baryons.

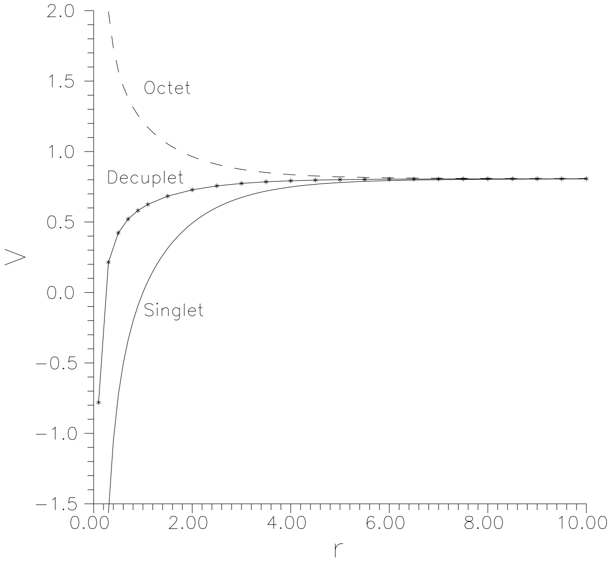

Fig. 8. The three-quark potential $V_1^{(QQQ)}(r,T)$ (in GeV) in different colour states for quarks placed at the vertices of an equilateral triangle with sides $r$ versus $r$ (in GeV$^{-1}$).

Similarly to the case of the quark–antiquark meson discussed in detail before the bound-state problem for a generic multiquark(gluon) system can be formulated in the form (we introduce the einbein variables $\mu_i$ for quarks and gluons):

$$H\psi_n=\varepsilon_n\psi_n,\quad H=H_0+H_S+H_{SE}, \tag{115}$$

where

$$H_0=\sum_{i=1}^{n_Q+n_g}\frac{\boldsymbol{p}_i^2}{2\mu_i}+V_1^{(n_Qq,n_gg)}(\boldsymbol{r}_{ij}) \tag{116}$$

and $H_S, H_{SE}$ are the spin-dependent and self-energy parts of Hamiltonian defined in terms of field correlators. Then the mass of the system is given by

$$M_n=\min_{\mu}\left\{\sum_{i=1}^{n_Q+n_g}\left(\frac{m_i^2}{2\mu_i}+\frac{\mu_i}{2}\right)+\varepsilon_n(\mu_1,...\mu_{n_Q+n_g})+\bar{a}V_1^{(Q\bar{Q})}(\infty,T)\right\}, \tag{117}$$

after the minimisation performed with respect to all einbeins $\{\mu_i\}$. The stationary values $\{\mu_i^{(0)}\}$ play the role of the constituent masses. In [46] a search for bound quark–antiquark states was performed in the potential given by the sum of the nonperturbative colour-electric interaction and the screened Coulomb interaction (see (74), (80), (82) above and the discussion in [46]),

$$V_1^{Q\bar{Q}}(r,T)=V_1^{\rm np}(r,T)+V_1^C(r,T). \tag{118}$$

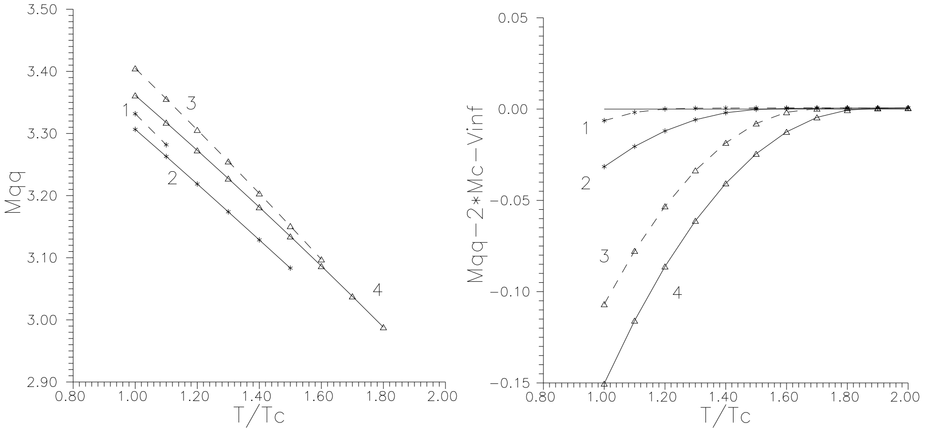

Fig. 9. Masses (first plot) and binding energies (second plot) of the $c\bar{c}$ colour-singlet bound states (in GeV) as functions of $T/T_c$. The curves are numbered in accordance with the data sets.

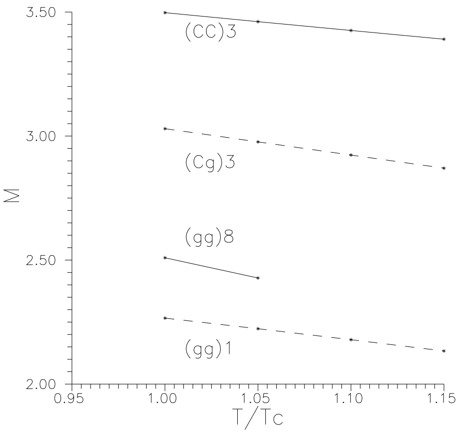

Fig. 10. Masses of bound states (in GeV) for the systems $(c\bar{c})_3$, $(cg)_3$, $(gg)_1$, and $(gg)_8$ as functions of $T/T_c$.

For the gluelump mass $M_0$ and the Debye mass — see (80) and (82) — several data sets were used: in set I $M_0 = 1.0$ GeV, $m_D$=0.69 GeV, in set II $M_0 = 1.0$ GeV, $m_D$=0.2 GeV, in set III $M_0 = 0.69$ GeV, $m_D$=0.69 GeV, in set IV $M_0 = 0.69$ GeV, $m_D$=0.2 GeV, in set V $M_0 = 1.044$ GeV, $m_D$=0.2 GeV, and in set VI $M_0 = 1.044$ GeV, $m_D$=1.044 GeV. The results are presented at Figs. 9, 10. From these figures one can see that, indeed, colour-electric interactions above the deconfinement temperature are strong enough to maintain bound states of quarks and gluons. Further details of the calculations can be found in [46].

### 4.2. Bound states at $T > T_c$ due to colour-magnetic forces

In this chapter we investigate bound states of quarks (generalisation to gluons is trivial) above the $T_c$ which appear due to the residual nonperturbative colour-magnetic interactions. We follow [13].

We start from the Hamiltonian of a quark–antiquark meson (40). Two particular cases are of most interest. The first such case corresponds to equal masses ($m_1 = m_2 = m$ and therefore $\mu_1 = \mu_2 = \mu$), whereas in the other case one mass is assumed infinitely large ($m_1 \to \infty$, $m_2 = m$ and $\mu_1 \to \infty$, $\mu_2 = \mu$). Then the Hamiltonian reads:

$$H = \frac{1}{\xi}\left(\frac{p_r^2+m^2}{\mu}+\mu\right)+\int_0^1 d\beta\left(\frac{\sigma_1^2 r^2}{2\nu}+\frac{\nu}{2}+\sigma_2 r\right)+\frac{\boldsymbol{L}^2}{r^2[\xi\mu+2\int_0^1 d\beta\nu(\beta-\xi/2)^2]}, \tag{119}$$

where $\xi = 1$ for the case of equal masses and $\xi = 2$ for the case of the heavy–light system.

We take the extrema in $\nu(\beta)$ and $\eta(\beta)$ now, approximating $\eta(\beta)$ by a uniform in $\beta$ distribution. Then the Hamiltonian (119) takes the form

$$H = \frac{1}{\xi}\left(\frac{p_r^2+m^2}{\mu}+\mu\right)+V_{\rm SI}(r), \tag{120}$$

and the spin–independent potential reads:

$$V_{\rm SI}(r) = \eta_0\sigma_E r+\left(\frac{1}{\eta_0}-\eta_0\right)\sigma_H r+\frac{1}{\xi}\mu y^2, \quad \eta_0=\frac{y}{\arcsin y}, \tag{121}$$

with $y$ being the solution of the transcendental equation

$$\frac{\sqrt{L(L+1)}}{\sigma_H r^2} = \frac{\xi}{4y}\left(1+\eta_0^2\left(1-\frac{\sigma_E}{\sigma_H}\right)\right)\left(\frac{1}{\eta_0}-\sqrt{1-y^2}\right)+\frac{\mu y}{\sigma_H r}. \tag{122}$$

The interested reader can find the details of a similar evaluation performed for the Hamiltonian (119) with $\sigma_E = \sigma_H = \sigma$ in [25,55].

The remaining einbein $\mu$ is to be considered as the variational parameter to minimise the spectrum of the Hamiltonian (120). Obviously, the extremal value of $\mu$ depends on quantum numbers and acquires two contributions: one coming from the current quark mass $m$ and the other, purely dynamical, contribution coming from the mean value of the radial component of the momentum $p_r$.

It is instructive to pinpoint the difference in the potential (121) below and above the $T_c$. At small $r$'s, the potential (121) turns to the centrifugal barrier $L(L+1)/(\xi\mu r^2)$, whereas its large–$r$ behaviour differs dramatically for the temperatures below and above the $T_c$. Indeed, the leading large-$r$ contribution to the inter-quark potential corresponds to $y \ll 1$ and, for $T < T_c$, reads:

$$V_{\rm conf}(r) = \sigma_E r. \tag{123}$$

This is the linear confinement which is of a purely colour–electric nature and which admits angular–momentum–dependent corrections (see [21,25]).

In the deconfinement phase, at $T > T_c$, the colour–electric part of the potential (121) vanishes, the leading long–range term coming from the angular–momentum–dependent part of the interaction:

$$V_{\rm SI}(r) = \frac{3L(L+1)}{\xi^2\sigma_H r^3} + \ldots. \tag{124}$$

Interestingly, in the deconfinement phase in absence of the confining potential, the spin–independent interaction becomes short–ranged decreasing as $1/r^3$ at large inter-quark separations. This feature means the full compensation of the centrifugal barrier which would naively behave as $1/r^2$ instead. The reason is obvious: at large inter-quark separations, the effective quark mass $\mu$ is to be compared to the "mass" of the string $\sigma r$. The bound–state problem solved in the potential (123) gives a large value $\langle p_r\rangle \propto \sigma_E\langle r\rangle$, so that, even for light (massless) quarks, their effective mass $\mu$ appears quite large ($\mu \gg m$). On the contrary, for light quarks and in absence of the strong confining interaction (123), the values of $\mu$ are small ($\mu \approx m$) and can be neglected as compared to the string contribution $\sigma_H r$. This makes the spin–dependent terms in the effective inter-quark interaction important in this regime, as opposed to the confinement phase, where they give only small corrections to the bound states formed in the confining potential (123).

Now we turn to the derivation of spin–dependent contributions to the inter-quark potential. The full set of spin-dependent interactions is given in (43). The leading spin–dependent term is the spin–orbit interaction (we omit contributions of $D_1^{E,H}$ which bring about short–range terms $\mathcal{O}(r^{-3})$),

$$V_{SO}(r) = \left(\frac{\boldsymbol{S}_1\boldsymbol{L}_1}{2\mu_1^2} - \frac{\boldsymbol{S}_2\boldsymbol{L}_2}{2\mu_2^2}\right)\left(\frac{1}{r}\frac{dV_0}{dr} + \frac{2}{r}\frac{dV_1}{dr}\right), \tag{125}$$

where $V_i(r)$ can be expressed through the colour–electric and colour–magnetic field correlators,

$$\frac{1}{r}\frac{dV_0}{dr} = \frac{2}{r}\int_0^\infty d\tau\int_0^r d\lambda D^E(\tau,\lambda), \quad \frac{2}{r}\frac{dV_1}{dr} = -\frac{4}{r}\int_0^\infty d\tau\int_0^r d\lambda\left(1-\frac{\lambda}{r}\right)D^H(\tau,\lambda). \tag{126}$$

Only the $V_1$ potential survives above the $T_c$, so that the resulting spin–dependent potential reads:

$$V_{SO}(r) = -\frac{2\xi\boldsymbol{SL}}{\mu r(\xi\mu + 2\langle\nu(\beta-\xi/2)^2\rangle)}\int_0^\infty d\tau\int_0^r d\lambda D^H(\tau,\lambda)\left(1-\frac{\lambda}{r}\right), \tag{127}$$

where

$$\langle\nu(\beta-\xi/2)^2\rangle \equiv \int_0^1 d\beta\nu(\beta-\xi/2)^2 = \frac{\sigma_H r}{2\xi^2 y^2}\left(1+\eta_0^2\right)\left(\frac{1}{\eta_0} - \sqrt{1-y^2}\right), \tag{128}$$

and $\boldsymbol{S} = \boldsymbol{S}_1 + \boldsymbol{S}_2$, for the light–light system, and $\boldsymbol{S}$ is the light–quark spin, for the heavy–light quarkonium.

It follows from (127) that above the deconfinement temperature, for the states with the total momentum $J = L + S$, $\boldsymbol{SL} > 0$ and the potential $V_{SO}(r)$ becomes

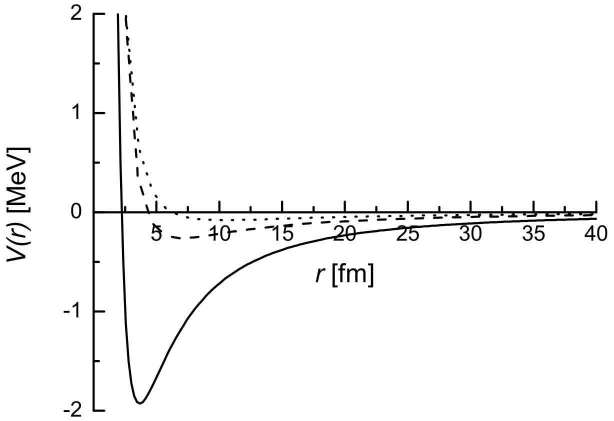

Fig. 11. The profile of the effective potential (130) for $m = 1$ GeV (solid line), $m = 2$ GeV (dashed line), and $m = 3$ GeV (dotted line).

attractive, with a possibility to maintain bound states. Furthermore, its slow decrease as $r \to \infty$ suggests that an infinite number of bound states exists, with the binding energies asymptotically approaching zero. Let us study these bound states in more detail. Hereafter in this chapter $\sigma_E = 0$ and we use the notation $\sigma$ for the magnetic tension $\sigma_H$.

In view of an obvious similarity of the light–light and heavy–light cases (the difference manifesting itself only in numerical coefficients), we investigate numerically only the light–light system, as a paradigmatic example. Furthermore, for $r \gg T_g$, the potential (127) does not depend on the form of the correlator $D^H$ since

$$2\int_0^\infty d\tau \int_0^r d\lambda D^H(\tau,\lambda)\left(1-\frac{\lambda}{r}\right) \underset{r\gg T_g}{\approx} \sigma. \tag{129}$$

Finally, we neglect the perturbative part of the inter-quark interaction for it is screened to a large extent contributing to short–ranged forces only whereas the effect discussed in this work is essentially a long–ranged effect.

Therefore we study the spectrum of bound states in the potential

$$V(r) = \left(\frac{\arcsin y}{y} - \frac{y}{\arcsin y}\right)\sigma r + \mu y^2 - \frac{\sigma l}{\mu r(\mu + 2\langle \nu(\beta - 1/2)^2\rangle)}, \tag{130}$$

which is the sum of the spin–independent term (121) and the spin–orbital term (127); $y$ is the solution of (122) with $\sigma_E = 0$. In Fig. 11 we plot the effective potential (130) for three values of the quark mass: $m = 1$GeV, 2GeV, and 3GeV.

The resulting eigenenergy $\varepsilon_{n_r l}(\mu)$ is added then to the free part of the Hamiltonian (119),

$$M_{n_r l}(\mu) = \frac{m^2}{\mu} + \mu + \varepsilon_{n_r l}(\mu), \tag{131}$$

| Parameter | $m_b$, GeV | $m_c$, GeV | $m_s$, GeV | $\sigma$, GeV$^2$ | $T_g$, fm |
|---|---|---|---|---|---|
| Value | 4.8 | 1.44 | 0.22 | 0.2 | 0.2 |

Table 2. The set of parameters used for the numerical evaluation.

| | $b\bar{b}$ | $c\bar{c}$ | $s\bar{s}$ |
|---|---|---|---|
| $n_r = 0$ | -0.007 | -0.19 | -45 |
| $n_r = 1$ | -5×10$^{-4}$ | -0.015 | -2.7 |

Table 3. The binding energy $E_{n_rL} \equiv M_{n_rL} - 2m$ (in MeV) for the ground state and for the first radial excitation in the potential (130) with $L = 1$ for the $b\bar{b}$, $c\bar{c}$, and $s\bar{s}$ quarkonia.

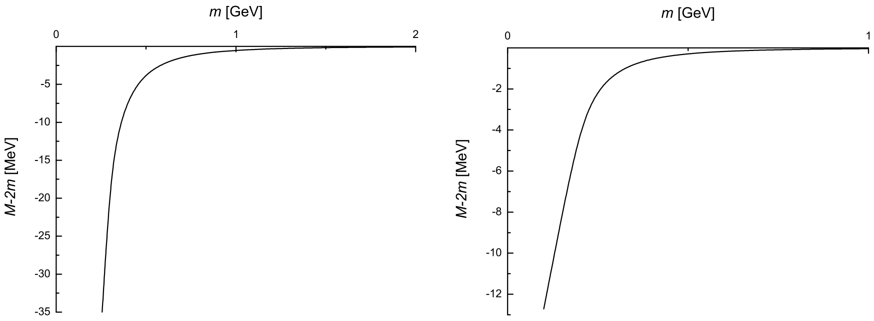

Fig. 12. The binding energy of the quark–antiquark system versus the mass of the quark for $L = 1$ and $n_r = 0$ (first plot) and $n_r = 1$ (second plot).

and this sum is minimised with respect to the einbein $\mu$,

$$\left.\frac{\partial M_{n_rl}(\mu)}{\partial \mu}\right|_{\mu=\mu_0} = 0, \quad M_{n_rl} = M_{n_rl}(\mu_0). \tag{132}$$

In Table 2 we present the set of parameters used in our numerical calculations, whereas in Table 3 we give the results for the binding energy for the $b\bar{b}$, $c\bar{c}$, and $s\bar{s}$ quarkonia above the $T_c$ for $l = 1$ and $n_r = 0, 1$. We ensure therefore that for $L \neq 0$ the potential (130) does support bound states. The binding energy is small ($|E_{n_rL}| \ll T$ for the $b$ and $c$ quarks and $|E_{n_rL}| \lesssim T$ for $s$ quarks) so these bound states can dissociate easily.

Let us discuss the problem of binding of light quarks. The effective potential (130) admits different forms at different inter-quark separations, depending on which contribution, of the quark mass term $\mu$ or of the "string mass" $2\langle\nu(\beta-1/2)^2\rangle$), gives the dominating contribution, that is for $\mu \gg \sigma r$ and $\mu \ll \sigma r$. If large distances contribute most to the bound state formation (the latter case), then $V(r) = \mathcal{O}(L(L+1)/(\sigma r^3)) + \mathcal{O}(L/(\mu r^2))$, where the first term comes from the spin-independent interaction (see (126)) and the other stems from the spin–orbit potential. The dependence of the binding energy on $\mu$ is expected then to be rather moderate, approximately as $1/\mu$.

On the contrary, in the former case with the string dynamics giving a correction to the quark mass term, the potential (130) can be approximated as

$$V(r) \approx \frac{L(L+1)}{\mu r^2} - \frac{\sigma l}{\mu^2 r}, \tag{133}$$

that is by the sum of the centrifugal barrier and the attractive Coulomb-like potential with the effective coupling

$$\alpha_{\rm eff} = \frac{\sigma L}{\mu^2}. \tag{134}$$

The corresponding eigenenergy can be found in any textbook in Quantum Mechanics and gives a stronger dependence on $\mu$,

$$\varepsilon(\mu) \propto -\mu\alpha_{\rm eff}^2 \propto -\frac{\sigma^2 L^2}{\mu^3}. \tag{135}$$

Let us consider the states with $L = 1$ and $n_r = 0$. We follow now the procedure described in detail before, that is we solve the full problem numerically, and find the dependence of the eigenenergy $\varepsilon$ on the einbein $\mu$ to be

$$\varepsilon(\mu) \propto -\frac{1}{\mu^{2.79}}. \tag{136}$$

Comparing this to (135) we find a good agreement, with the small deviation in the power resulting from the proper string dynamics. We conclude therefore that the dynamics of the system develops at the inter-quark separations $T_g \ll r \lesssim m/\sigma$ (since, for the set of parameters given in Table 2, $m \gtrsim \sigma T_g$ then there is room for such separations).

Let us discuss now the procedure of minimisation of the spectrum (131) in $\mu$. First of all, let us notice that, in the einbein field formalism, the calculation of the spectrum naively looks like a nonrelativistic calculation due to the "nonrelativistic" form of the kinetic energy in the Hamiltonian with the einbein field $\mu$ introduced. In the meantime, the full relativistic form of the quark kinetic energy is readily restored as $\mu$ takes its extremal value and hence this is the procedure of taking extremum in $\mu$ in the masses (131) to sum up an infinite series of relativistic corrections and thus to restore the relativistic spectrum. For example, the relativistic ground state eigenenergy $E_0 = m\sqrt{1-(Z\alpha)^2}$ of the one–body Dirac equation with the Coulomb potential $-Z\alpha/r$ can be reproduced *exactly* with the help of the einbein technique. Finally, one can visualise the form of $\mu$ considering the effective Dirac equation for the light quark in the field of the static antiquark source. When written in the form of a second–order differential equation, it contains the spin–orbit term of the same form as given in (125) but with $\mu$ replaced by the combination $\epsilon + m + U - V$, where $U$ and $V$ are scalar and vector potentials, respectively. For light (massless) quarks this combination takes drastically different values below and above the deconfinement temperature. Indeed, in the confining phase of QCD, when spontaneous chiral symmetry breaking leads to a strong effective, dynamically generated scalar potential $U$, this effective "$\mu$" is large. On the contrary, above the $T_c$, when $U$ is small "$\mu$" is also small (it can be even negative since the eigenenergy $\epsilon$ may have any sign).

It has been found numerically that the extremum in $\mu$ for $M_{n_rL}(\mu)$, (131), exists for $m$ exceeding the value of approximately 0.22GeV (for the given $\sigma = 0.2$GeV), and no extremum exists for smaller values of the quark mass (see Fig. 12 for the dependence of the binding energy $E_{n_rL}$ on the quark mass). This property of the bound state spectrum can be easily understood using the analogy with the bound state problem for the Dirac equation with the potential in the form of a deep square well or Coulomb potential discussed above. For example, for the Coulomb potential, a problem appears as the coupling exceeds unity — the well–known problem of $Z > 137$. From (134) we easily find this critical phenomenon to happen at $m \approx \mu \lesssim \sqrt{\sigma} \approx 0.4$GeV. This estimate is in good agreement with the result of our direct numerical calculations quoted above.

Physically this situation means that many quark–antiquark and/or gluon pairs are formed and finally stabilise the vacuum. Formally the problem is not anymore a two–body problem, but rather many–body, so that many–body techniques are to be applied. For example, in electrodynamics with $Z > 137$, one can derive the resulting self-consistent field of the Thomas–Fermi type [56]. A similar situation can be expected in the deconfinement phase of QCD. In absence of the linear potential, the einbein $\mu$ (playing the role of the effective quark mass) is not anymore bounded from below by the values of order $\sqrt{\sigma_E} \simeq 0.4$GeV coming from the binding energy in the linearly rising potential. To see the onset of this phenomenon in the framework of our two–body (one–body for the heavy–light case) Hamiltonian, one should take into account the negative–energy part of the spectrum, when the full matrix form of the Hamiltonian is considered [57]. Indeed, the matrix structure of the Hamiltonian occurs in the path–integral formalism from the two–fold time–forward/backward motion described by the positive/negative values of $\mu$. Off–diagonal terms in the matrix Hamiltonian produce the turning points in the particle trajectory and result in Z–graphs.

Notice that the same is true for the glueballs and gluelumps since in this case equations are the same as for light–light and heavy–light quarkonia, respectively, but with the quark spin replaced by the gluon spin and $\sigma_H$ by $\frac{9}{4}\sigma_H$.

It is important to notice that a separated quark–antiquark pair was considered in this chapter. In reality such quark–antiquark pairs are to be considered in the medium formed by other quarks and gluons, that is as a part of the SQGP. As a measure of the interaction in SQGP one can consider the ratio of the mean potential energy to the mean kinetic energy of the particles in the plasma, $\Gamma = \langle V\rangle/\langle K\rangle$. It is easy to estimate that $\langle K\rangle \simeq T$ and $\langle V\rangle \simeq \sigma_H/T$. This gives $\Gamma = \sigma_H/T^2$ and so this parameter is large for quarks and it is several times larger for gluons. Therefore, SQGP is a strongly interacting medium which looks like a liquid, rather then as a gas. With the growth of the temperature the medium becomes more dense, and the mean distance between particles decreases. As this distance becomes comparable to the radius of the bound states discussed in this chapter, the latter will dissociate because of the screening effects. In other words, the hot medium plays the role of a natural cut–off for the effect of bound pair creation discussed above. Notice however that, for the quark masses around 0.2GeV, the radius of the bound state is of the order of one fm and it is expected to decrease further with the decrease of the quark mass, even if the pair creation process is properly taken into account. This means that indeed there is room for such bound states for the temperatures above the $T_c$. Breakup, with the growth of the temperature, of such high–$l$ states for quarks, and especially for gluons which possess more degrees of freedom than quarks, may affect such characteristics of the plasma as its free energy and it entropy (for a recent paper of explaining the near–$T_c$ behaviour of these characteristics see [58]).

Concluding this section one can say that colour–magnetic (spin–dependent) interaction acting on light quark or gluonic systems enforces nonperturbative creation of light $q\bar{q}$ and $gg$ pairs.

## 5. Generalisation to nonzero baryon densities

In this section we will extend the method to the case of nonzero $\mu$ and nonzero interaction with vacuum ($V_1 \neq 0$) and to find $T_c(\mu)$, for $\mu > 0$. The simple picture of VD dynamics with the only input $L_{\rm fund}(T)$, taken from lattice or analytic calculation suggested in [35], which was discussed below as the Vacuum Dominance Model (VDM), is adopted below and is shown to produce surprisingly reasonable results, being in good agreement with available lattice data for nonzero $\mu$, where these data are reliable.

### 5.1. *Nonperturbative EoS for $\mu > 0$*

The main idea of the VDM is that the most important part of quark and gluon dynamics in the strongly interacting plasma is the interaction of each individual quark or gluon with vacuum fields. This interaction is derived from field correlators and is rigorously proved to be embodied in factors, which happen to coincide with the modulus of Polyakov loop[c],

$$L_{\rm fund} = \exp\left(-\frac{V_1(T)+2V_D}{2T}\right), \quad L_{\rm adj} = \exp\left(-\frac{9}{4}\frac{V_1(T)+2V_D}{2T}\right), \tag{137}$$

where $V_1(T) \equiv V_1(\infty, T)$, $V_D \equiv V_D(r^*, T)$ and $V_1(r,T), V_D$ found in [42] to be ($\beta \equiv 1/T$) the same as for $\mu = 0$ case (see Eqs. (73),(74)) but with $D^E$, $D_1^E$ in principle depending on $\mu$.

---

[c] We neglect in this approximation the difference between $L_{\rm fund}$ expressed via $V_1(\infty, T)$ and $L^{lat}_{\rm fund}$ where the role of $V_1(T)$ is played [35,42] by singlet $Q\bar{Q}$ free energy $F^1_{Q\bar{Q}}(\infty, T)$. The latter quantity contains all excited states, so that $V_1(T) \geq F^1_{Q\bar{Q}}(\infty, T)$.

In $V_D$, Eq.(137) $r^*$ is the average size of the heavy-light $Q\bar{q}$ or its adjoint equivalent system; for $T > T_c$ one has $D^E = V_D = 0$. For $T < T_c$ one has $r^*_{\rm fund} = \infty$ for $n_f = 0$, yielding $L_{\rm fund} = 0$, however $r^*_{\rm adj} \approx 0.4$ fm for any $n_f$ and gives nonzero $L_{\rm adj}(T < T_c)$. The form (137) is in good agreement with lattice data [33] and also explains why $L_{\rm fund}$ is a good order parameter (however approximate for $n_f \neq 0$). Note, that only NP parts $D^E_1, D^E$ enter in (73),(74), see [42] for discussion of separation of these parts; renormalisation procedure is discussed also in [46].

In the lowest NP approximation one neglects pair, triple etc. interactions between quarks and gluons (which are important for $T_c \le T \lesssim 1.2T_c$ where density is low and screening by medium is not yet operating, see [13,35])) and derives the following EoS (this approximation is called in [35,36] the Single Line Approximation (SLA))

$$p_q \equiv \frac{P^{SLA}_q}{T^4} = \frac{4N_c n_f}{\pi^2}\sum_{n=1}^{\infty}\frac{(-1)^{n+1}}{n^4}L^n_{\rm fund}\varphi^{(n)}_q \cosh\frac{\mu n}{T}, \tag{138}$$

$$p_{gl} \equiv \frac{P^{SLA}_{gl}}{T^4} = \frac{2(N^2_c-1)}{\pi^2}\sum_{n=1}^{\infty}\frac{1}{n^4}L^n_{\rm adj} \tag{139}$$

with

$$\varphi^{(n)}_q(T) = \frac{n^2 m^2_q}{2T^2}K_2\left(\frac{m_q n}{T}\right) \approx 1 - \frac{1}{4}\left(\frac{n m_q}{T}\right)^2 + \ldots \tag{140}$$

In (138), (139) it was assumed that $T \lesssim \frac{1}{\lambda} \cong 1$ GeV, where $\lambda$ is the vacuum correlation length, e.g. $D^{(E)}_1(x) \sim e^{-|x|/\lambda}$, hence powers of $L^n_i$, see [35] for details.

With few percent accuracy one can replace the sum in (139) by the first term, $n = 1$, and this form will be used below for $p_{gl}$, while for $p_q$ this replacement is not valid for large $\frac{\mu}{T}$, and one can use instead the form equivalent to (138),

$$p_q = \frac{n_f}{\pi^2}\left[\Phi_\nu\left(\frac{\mu - \frac{V_1}{2}}{T}\right) + \Phi_\nu\left(-\frac{\mu + \frac{V_1}{2}}{T}\right)\right] \tag{141}$$

where $\nu = m_q/T$ and

$$\Phi_\nu(a) = \int_0^\infty \frac{z^4 dz}{\sqrt{z^2+\nu^2}}\frac{1}{(e^{\sqrt{z^2+\nu^2}-a}+1)}. \tag{142}$$

Eqs. (141), (139) define $p_q, p_{gl}$ for all $T, \mu$ and $m_q$, which is the current (pole) quark mass at the scale of the order of $T$.

To draw $p_q, p_{gl}$ and $p \equiv p_q + p_{gl}$ as functions of $T, \mu$ one needs explicit form of $V_1(T)$. This was obtained analytically and discussed in [42]; another form was found from $D^E_1(x)$ measured on the lattice in [59] and is given in [46].

Also from lattice correlator studies [8,59] $V_1(T = T_c)$ is (with $\sim 10\%$ accuracy) 0.5 GeV and is decreasing with the growth of $T$ (cf. Fig. 2 of [42] and Fig. 1 of [46]). This behaviour is similar to that found repeatedly on the lattice direct measurement of $F^{(1)}_\infty$, see e.g. Fig. 2 of [45] where $F^{(1)}_\infty = V_1(T)$ is given for $n_f = 0, 2, 3$. In what

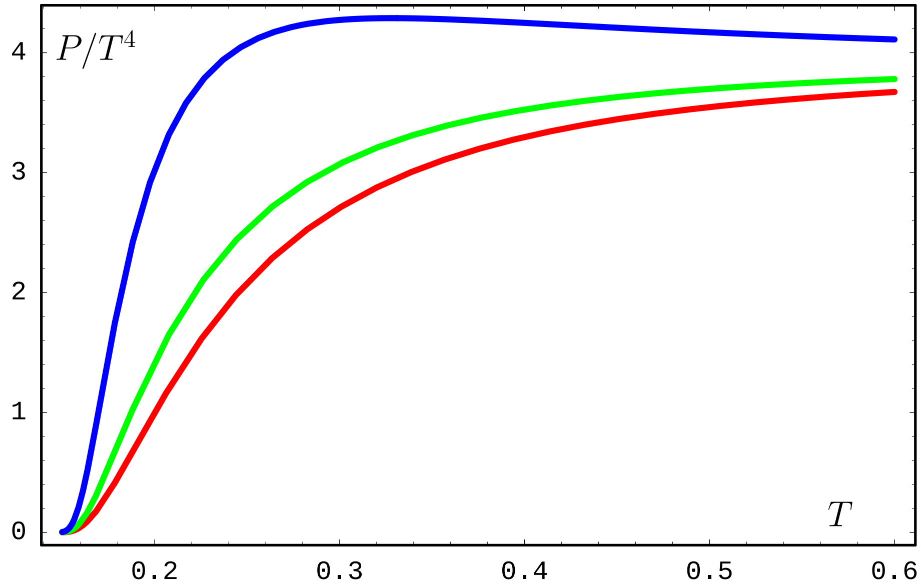

Fig. 13. Pressure $\frac{P}{T^4}$ from Eq.(138,139) as function of temperature $T$ (in GeV) for $n_f = 2$, $\mu = 0$, 0.2, 0.4 GeV (bottom to top), and $\Delta G_2 = 0.0034$ GeV$^4$.

follows we shall exploit the latter curves parameterizing them for $T \geq T_c$ and all $n_f$ as

$$V_1(T) = \frac{0.175 \text{ GeV}}{1.35 \left(\frac{T}{T_c}\right) - 1}, \quad V_1(T_c) \approx 0.5 \text{ GeV}. \tag{143}$$

For $\mu > 0$ one can expect a $\mu$-dependence of $V_1$, however it should be weak for values of $\mu$ much smaller than the scale of change of vacuum fields. The latter scale can be identified with the dilaton mass $m_d$, which is of the order of the lowest glueball mass, i.e. $\sim 1.5$ GeV $\equiv m_d$. Hence one can expect, that $V_1$ in the lowest approximation does not depend on $\mu$. This is supported by the lattice measurements in [60], where for $\frac{T}{T_c} = 1.5$ and $\frac{\mu}{T} = 0.8$ the values of $F_\infty^{(1)}$ are almost indistinguishable from the case of $\frac{\mu}{T} = 0$.

To give an illustration of the resulting EoS we draw in Fig. 13 the pressure $p$ for the cases $\mu = 0$, 0.2, 0.4 GeV and $n_f = 2$. One can see a reasonable behaviour similar to the lattice data, see [61] for a review and discussion.

### 5.2. *Phase transition for nonzero $\mu$*

Here we extend the VD mechanism suggested in [9] to the case of nonzero $\mu$ and $V_1$. We assume as was said in Introduction that the phase transition occurs from the full confining vacuum with all correlators $D^E, D_1^E, D^H, D_1^H$ present to the deconfined vacuum where $D^E$ vanishes. The basics of our physical picture is that all fields (and correlators) do not change for $\mu, T$ changing in a wide interval, unless $\mu, T$ become comparable to the dilaton mass $m_d \approx M(\text{glueball } 0^+) \approx 1.5$ GeV[d]. Therefore correlators and $\sigma^E, \sigma^H$ are almost constant till $T = T_c$ and at $T \geq T_c$ a new vacuum phase with $D^E = \sigma^E = 0$ is realised, which yields lower thermodynamic potential (higher pressure). Lattice measurements [8,59] support this picture. The crucial step is that one should take into account in the free energy $F$ of the system also the free energy of the vacuum, i.e. vacuum energy density $\varepsilon_{vac} = \frac{1}{4}\theta_{\mu\mu} = \frac{\beta(\alpha_s)}{16\alpha_s}\langle (F^a_{\mu\nu})^2\rangle = -\frac{(11-\frac{2}{3}n_f)}{32}G_2$, which can be estimated via the standard gluonic condensate [62] $G_2 \equiv \frac{\alpha_s}{\pi}\langle (F^a_{\mu\nu})^2\rangle \approx 0.012$ GeV$^4$.

Hence for the pressure $P = -F$ one can write in the phase $I$ (confined)

$$P_I = |\varepsilon_{vac}| + \chi_1(T) \tag{144}$$

where $\chi(T)$ is the hadronic gas pressure, starting with pions, $\chi_{pion} \cong \frac{\pi^2}{30}T^4$. In the deconfined phase one can write

$$P_{II} = |\varepsilon^{dec}_{vac}| + (p_{gl} + p_q)T^4 \tag{145}$$

where $|\varepsilon^{dec}_{vac}|$ is the vacuum energy density in the deconfined phase, which is mostly (apart from $D^E_1(0) \approx 0.2D^E(0)$, see [8,63]) colourmagnetic energy density and by the same reasoning as before we take it as for $T = 0$, i.e. $|\varepsilon^{dec}_{vac}| \cong 0.5|\varepsilon_{vac}|$.

Equalizing $P_I$ and $P_{II}$ at $T = T_c(\mu)$ one obtains the equation for $T_c$

$$T_c(\mu) = \left(\frac{\Delta|\varepsilon_{vac}| + \chi(T)}{p_{gl} + p_q}\right)^{1/4} \tag{146}$$

where $\Delta|\varepsilon_{vac}| = |\varepsilon_{vac}| - |\varepsilon^{dec}_{vac}| \approx \frac{(11-\frac{2}{3}n_f)}{32}\Delta G_2;\ \ \Delta G_2 \approx \frac{1}{2}G_2$; $p_{gl}$ and $p_q$ are given in (139), (141) respectively and depend on both $T_c$ and $\mu$.

In this letter we shall consider the simplest case when the contribution of hadronic gas $\chi_1(T)$ can be neglected in the first approximation. Indeed, pionic gas yields only $\sim 7\%$ correction to the numerator of (146) at $T \approx T_c$, and from [64] one concludes that $\chi(T_c) \lesssim 0.5T_c^4$, which yields a $\lesssim 10\%$ increase of $T_c$ for $G_2 \sim 0.01$ GeV.

From the expression for $T_c(\mu)$ (146) one can find limiting behaviour of $T_c(\mu \to 0)$ and $\mu_c(T \to 0)$. For the first one can use for $p_q$ and $p_g$ (138) and (139) and expand r.h.s. of (146) in ratio $p_g/p_q$ with the result.

$$T_c = T^{(0)}\left(1 + \frac{V_1(T_c)}{8T_c} + O\left(\left(\frac{V_1(T_c)}{8T_c}\right)^2\right)\right) \tag{147}$$

---

[d] Note that $G_2$ does not depend on $\mu, n_f$ in the leading order of the $1/N_c$ expansion and one expects a growth of the magnetic part of $G_2$ at $T > T_{dim.red} \approx 2T_c$, $G_2^{mag} \approx O(T^4)$, in the regime of dimensional reduction.

where the last term yields a 3% correction, and $T^{(0)} = \left(\frac{(11-\frac{2}{3}n_f)\pi^2\Delta G_2}{32\cdot 12 n_f}\right)^{1/4}$. Solving (147) for $T_c$ one has

$$T_c = \frac{1}{2}T^{(0)}\left(1+\sqrt{1+\frac{\kappa}{T^{(0)}}}\right)\left(1+\frac{m_q^2}{16T_c^2}\right) \qquad (148)$$

with $\kappa \equiv \frac{1}{2}V_1(T_c)$. From (146), (147) one can compute expansion $T_c(\mu)$ in powers of $\mu$,

$$T_c(\mu_B) = T_c(0)\left(1 - C\frac{\mu_B^2}{T_c^2(0)}\right), \quad \mu_B = 3\mu.$$

$$C = \frac{1+\sqrt{1+\frac{\kappa}{T^{(0)}}}}{144\sqrt{1+\frac{\kappa}{T^{(0)}}}} = 0.0110(3) \ \text{ for } n_f = 2,3,4.$$

One can see, that $C$ practically does not depend on $n_f$ and is in the same ballpark as the values found by lattice calculations, see [65,66] for reviews and references.

Another end point of the phase curve, $\mu_c(T\to 0)$, is found from (146) when one takes into account asymptotic $\Phi_0(a\to\infty) = \frac{a^4}{4} + \frac{\pi^2}{2}a^2 + \frac{7\pi^4}{60} + ...$, which yields (for small $\frac{m_q}{\mu}$)

$$\mu_c(T\to 0) = \frac{V_1(T_c)}{2} + (48)^{1/4}T^{(0)}\left(1+\frac{3m_q^2}{4\mu_c^2}\right)\left(1-\frac{\pi^2}{2}\frac{T^2}{\left(\mu_c - \frac{V_1(T_c)}{2}\right)^2}\right) \qquad (149)$$

The resulting curve $T_c(\mu)$ according to Eq.(146) with $\chi_1 \equiv 0$ is given on Fig. 14 (left side) for $\Delta G_2 = 0.00341\text{GeV}^4$, $n_f = 2,3$ and $m_q = 0$. To compare, we have shown on the same figure (right side) the lattice data [67] obtained in the reweighting technique.

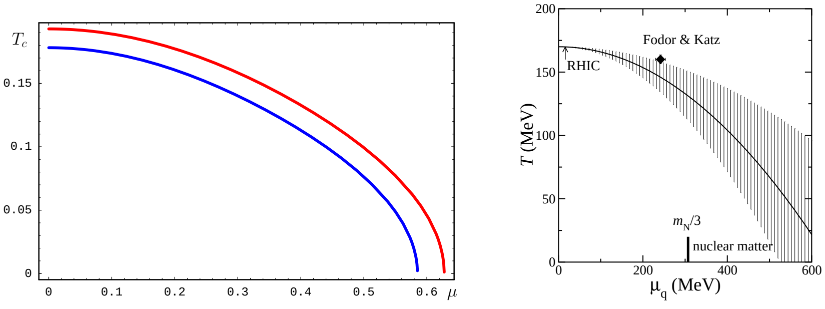

Fig. 14. The phase transition curve $T_c(\mu)$ from Eq.(146) (in GeV) as function of quark chemical potential $\mu$ (in GeV) for $n_f = 2$ (upper curve ) and $n_f = 3$ (lower curve) and $\Delta G_2 = 0.0034$ GeV$^4$ (left side) in comparison with lattice results [67] (right side)

.

Table 4. The values of $T_c(\mu = 0)$ and $\mu_c(T = 0)$ computed using (148) and (149) for several values of $\Delta G_2$ and $n_f = 0, 2, 3$.

| $\Delta G_2/(0.01\ \text{GeV}^4)$ | 0.191 | 0.341 | 0.57 | 1 |
|---|---|---|---|---|
| $T_c$(GeV) $n_f = 0$ | 0.246 | 0.273 | 0.298 | 0.328 |
| $T_c$(GeV) $n_f = 2$ | 0.168 | 0.19 | 0.21 | 0.236 |
| $T_c$(GeV) $n_f = 3$ | 0.154 | 0.172 | 0.191 | 0.214 |
| $\mu_c$(GeV) $n_f = 2$ | 0.576 | 0.626 | 0.68 | 0.742 |
| $\mu_c$(GeV) $n_f = 3$ | 0.539 | 0.581 | 0.629 | 0.686 |

### 5.3. *Discussion of results*

The prediction of $T_c(\mu)$ depends only on two numbers: 1) the value of gluonic condensate $\Delta G_2$ and 2) the value of $V_1(T_c) = 0.5$ GeV taken from lattice data [45] (and quantitatively close to the value from the analytic form [42]).

We take $G_2$ in the limits $0.004\ \text{GeV}^4 \le G_2 \le 0.015\ \text{GeV}^4$, the value $G_2 = 0.008\text{GeV}^4$ ($\Delta G_2 = 0.0034\ \text{GeV}^4$) being in agreement with lattice data of $T_c(0)$, for $n_f = 0, 2, 3$, see Table 4.

Note that $T_c$ at $n_f = 0$ in Table 4 is obtained not from (148), but directly from (146) with $n_f = 0, \chi(T) = 0$.

The curve in Fig. 14 has the expected form, which agrees with the curve, obtained in [67] by the reweighting technique and agrees for $\mu < 300$ MeV with that, obtained by the density of state method [68], and by the imaginary $\mu$ method [61].

An analysis of the integral (142) for $\nu = 0$ reveals that it has a mild singular point at $\mu_{sing} = \frac{V_1}{2} \pm i\pi T$, which may show up in derivatives in $\frac{\mu}{T}$. At $T = 0, \mu_{sing} = \frac{V_1}{2} \cong 0.25$ GeV and is close to the point where one expects irregularities on the phase diagram [68,69].

The limit of small $\mu$ is given in (148). Taking $V_1(T_c) \approx 0.5$ GeV as follows from lattice and analytic estimates, one obtains with $\sim 3\%$ accuracy the values of $T_c$ given on Fig. 14 for $n_f = 2, 3$ and $\Delta G_2 = 0.0034\ \text{GeV}^4$.

The values of $\mu_c$, from (149) are given in Table 4 and are in agreement with the curves shown in Fig. 14. Note that $\chi(T=0)=0$ and (149) holds also in the case, when hadron (and baryon) gas is taken into account.

At this point one should stress that our calculation in VDM of $p(T)$ does not contain model parameters and the only approximation is the neglect of interparticle interaction as compared to the interaction of each one with the vacuum (apart from neglect of $\chi(T)$). Fig. 13 demonstrates that this approximation is reasonably good and one expects some 10÷15% accuracy in prediction of $T_c(\mu)$. Note that in VDM the phase transition is of the first order, which is supported for $n_f=0$ by lattice data, see e.g. [33] however for $n_f=2,3$ lattice results disagree, see [70,71] for a possible preference of the first order transition. One however should have in mind that the final conclusion for lattice data depends on input quark masses and continuum limit.

The "weakening" of the phase transition for $n_f>0$ and nonzero quark masses is explained in our approach by the flattening of the curve $P(T)$ at $T\approx T_c$ when hadronic gas $\chi(T)$ is taken into account, since $\chi(T)$ for $n_f=0$ is much smaller than for $n_f=2$.

Finally, as seen from our expressions for $p_q, p_g$ (138), (141), our EoS is independent of $Z(N_c)$ factors and $Z(N_c)$ symmetry is irrelevant for the NP dynamics in our approach. This result is a consequence of more general property − the gauge invariance of the partition function for all $T$, $\mu$, which requires that only closed Wilson loops appear in the resulting expressions, yielding finally only absolute value of the Polyakov loop, or in other words, is expressed via only singlet free energy of quark and antiquark $F^{(1)}_{Q\bar{Q}}\approx V_1$.

## 6. Concluding discussions

### 6.1. *Comparison to other approaches*

Our resulting EoS, in particular $P(T,\mu)$ in the leading (single line) approximation has the form of ideal gas factors multiplied by moduli of Polyakov Lines (PL). In the next orders also interaction between quark and gluon lines is included, which leads to the decreasing of pressure, so the final results are in better agreement with lattice data, see Figs. 3–6.

The interaction between quarks and gluons has both colourelectric and colourmagnetic components and was discussed in section 4.

Thus it is clear that PL play a very important dynamical role in the FCM. This role is in creation of $T$-dependent self-energy term for each individual quark or gluon, which suppresses their contribution to the pressure. One can say therefore, that quarks and gluons acquire vacuum induced effective masses.

From this point of view it is reasonable to discuss other approaches in the literature, where PL play important role.

One should start with the formalism of effective action for Polyakov lines, existing for almost 30 years [72–74], see also [75] for later development.

Here PL and $Z(N)$ symmetry are mostly used conceptually as an order parameter for the deconfinement transition, and the effective potential was calculated for purely gluon and quark-gluon system to study potential extrema in terms of PL moduli and phases. From the discussion in sections 1-4 it is clear however, that only moduli of PL enter EoS in our approach and $Z(N)$ symmetry is irrelevant for dynamical properties of QGP. Moreover, quarks violate $Z(N)$ symmetry and the latter has no connection with the deconfinement in the unquenched case. Instead, moduli of PL are crucially important as dynamical input in establishing EoS and the QCD phase diagram at nonzero $\mu$.

Indeed, it is the modulus of $L(T)$, which defines in Eq. (146) the transition temperature $T_v(\mu)$ in the SLA.

There is another approximation [76,77] in the theory of QGP, which is closer to ours, since it also uses PL as a kind of dynamical input. It is called PNJL and is based on the Nambu-Jona-Lasinio Lagrangian with quark operators augmented by PL. Here one obtains EoS and effective quark and gluon masses in qualitative agreement with lattice data. However, since NJL Lagrangian is not confining, the detailed picture of deconfinement may be quite different.

The action density of the PNJL model can be written as (see Rössner et al in [77] for a review and additional references)

$$S = \psi^+(\partial_\tau - i\boldsymbol{\alpha}\nabla + \gamma_4 m_0 - A_4)\psi + N(\psi,\psi^+), \tag{150}$$

where $N$ is quartic in $\psi$ as in NJL model, and $A_4$ is constant field entering PL, which therefore become complex in general. This fact and the associated $Z(N_c)$ symmetry differs from our results and our EoS, where only modulus of PL enters. Nevertheless one can obtain in this approach a reasonable agreement for the first moments of pressure with respect to $\mu/T$ [77].

At this point it is useful to compare our results with the phenomenological models of QGP, where quark and gluon masses have been introduced as input and fitting parameters ,see e.g. [78,79].

In [78,79] the quasiparticle propagators are introduced with real and imaginary parts of self-energy (effective mass) terms, which can be compared to our PL self-energies, $\varepsilon_i = \frac{1}{2}c_i V_1(\infty,T)$, $L_i = \exp\left(-\frac{V_1(\infty,T)}{2T}c_i\right), \quad i = q,g, \quad c_i = 1, \frac{9}{4}$.

It is interesting that the resulting effective masses for quarks and gluons approximately satisfy Casimir scaling as in our $c_i V_1(\infty,T)$, and have the same order of magnitude as in our calculations. A more detailed comparison will be subject of future publications.

We now turn to the important question of the density induced phase transition, which may be important for several planned ion machines and possible existence of quark cores in neutron stars. As was discussed above in section 5, FCM predicts deconfinement phase transition at large $\mu_q = \mu_{cr} \approx 0.6$ GeV, provided vacuum properties and in particular gluon condensate and PL are not affected by $\mu_q$. It is important to study what happens in the region $\mu_N \leq \mu_q \leq \mu_{cr}$, where $\mu_N$ is the chemical potential at normal nuclear density, $\mu_N \approx 0.3$ GeV.

It is clear that nonzero $\mu_q$ can influence baryon structure, and some change in the nucleon mass and radius was studied before [80]. However much more drastic change due to $\mu_q$ appears in the interquark forces, as was found in [81]. Here it was realized that light quark interaction and confinement is obtained self-consistently from nonlinear equations, yielding linear scalar confinement for vanishing $\mu_q$, but a deeper well for $r < \frac{\mu_q}{\sigma}$ appears for nonzero $\mu_q$, which makes baryon lighter and more compact. Moreover, $3nq$ systems may become more stable for $n = 1, 2, ...$ due to larger number of pairing interquark forces. More detailed quantitative analysis is needed for the final positive answer, however it seems feasible , that at growing $\mu_q$ the nuclear matter becomes a dense medium of smaller size $3q$ with an admixture of $6q, 9q$,... bags, the latter is growing in percentage with $\mu_q$, unless quarks find themselves finally in the deconfined phase. In this scenario the role of multiquark bags and, hence, of cumulant mechanism is growing with density, which can be measured experimentally in future ion-ion experiments.

Till now nothing was said about $qq$ pairing and possible quark superconductivity, widely discussed in literature — see [82] for reviews. The $np$ vacuum changes this picture in several respects. The first one was discussed in [83], where it was stressed, that the minimum of thermodynamic potential $\Omega_0$ (with the gap in the scalar diquark sector $\Delta_0 = (0.1 \div 0.15)$ GeV is of the order of $10^{-3}$ GeV$^4$ or less, and this value is of the order of $np$ vacuum density $|\varepsilon|$, so the realization of the perturbative diquark condensation crucially depends on this $np$ value and is questionable when $|\Omega_0| < |\varepsilon|$.

Another $np$ feature of the QCD vacuum, which may prevent standard diquark scenario, is the $qq$ interaction in the diquark sector, discussed in section 4. As can be seen in Eq. (108) interaction in the $qq$ sector can be written as

$$V_{qq} = \bar{a}_d V_1(\infty, T) + \bar{b}_d V_1(r, T), \tag{151}$$

where $\bar{a}_{\bar{3}} = \frac{1}{2}, \ \ \bar{a}_6 = \frac{5}{4}, \ \ \bar{b}_{\bar{3}} = \frac{1}{2}, \ \ \bar{b}_6 = -\frac{1}{4}$ to be compared with $q\bar{q}$ system, where $\bar{a}_1 = 0, \ \ \bar{b}_1 = 1$ and $V_1(\infty, T_c) \approx 0.5$ GeV.

Here $V_1(r, T)$ is the sum of perturbative and $np$ interactions, $V_1(r, T) = V_1(\infty, T) + v(r, T)$, and $v_{np}(r, T)$ is negative everywhere.

As a result one has additional (constant) repulsion in the $qq$ system as compared to $q\bar{q}$, of the order of $\frac{1}{2} V_1(\infty, T_c) \approx 0.25$ GeV, which is larger than the assumed gap $\Delta_0$. Therefore one can expect that pairing is destroyed and one has only white correlations in the $q\bar{q}$ and $qqq$ systems which can appear as bound states, e.g. in the $S$ -wave $c\bar{c}$ system, which is supported by lattice data [84].

Thus we are coming again to the " quark-bag scenario" discussed above, where nucleons in nuclear matter become tighter and lighter with increasing density and are accompanied with growing number of $6q$, $9q$, ... quark bags finally occupying the whole volume.

This scenario possibly implies a more hard EoS of nuclear matter, than usually exploited and can lead to higher masses of neutron stars with quark matter cores, see in this respect the discussion in [85,86].

Finally, we discuss in interesting idea of Dremin and collaborators, about the possibility of Cherenkov emission of gluons in QGP due to the effective creation of nonzero dielectric permittivity $\varepsilon$ in a dense medium [87]. As was shown there, this Cherenkov emission can possibly explain the double-humped structure of the away-side jet at RHIC. We can add here from the point of view of FCM, that $\varepsilon$ is sensitive not only to the medium effects, but can also get contributions from the change of QCD vacuum properties, which happens at $T > T_c$. This topic is now under investigation.

### 6.2. *Mysteries of deconfinement*

The theory discussed in this review was able to address most important questions related to the QGP dynamics, namely:

(1) Why does deconfinement take place at some temperature and density? The theory based on the FCM shows that thermodynamic potential (pressure) grows faster with the temperature $T$ in the deconfined phase, as compared to the confined phase, so that the (almost) constant difference in vacuum energy density between the phases is overcome at some $T = T_c$.

(2) What is the main dynamical difference between the phases? It is shown in the review that, in the confined phase, both colourelectric (CE) and colourmagnetic (CM) confinement coexist while, in the deconfined phase, only the latter is retained [88]. In the meantime, CE forces due to the nonconfining correlator $D_1^E$ also survive in the deconfined phase and they can support bound states at not too large $T$'s, $T \lesssim 1.5T_c$.

(3) What are manifestations of the CM confinement? As was discussed in this review, the CM confinement ensures strong interaction in the quark-gluon systems and can support weakly bound states for nonzero angular momentum $L$. Moreover, most part of the spin-dependent forces is due to the CM confining correlator $D^H$ and thus it survives the deconfinement transition [89]. The CM confinement solves the old Linde paradox since the 3D perturbative diagrams acquire Wilson loops of the confining background field. The latter converge at large distances as $\langle W\rangle \sim \exp(-\sigma_H \times \text{area})$ and make all integrals convergent [10]. However, this is probably only a small part of the story. Indeed, the very notion of confinement implies that, when moving with some velocity, any coloured subsystem is not free but is rather connected, by a CM string, to its colour partner, which makes the entire system white. As a consequence, a gluon or a quark acquires a nonperturbative CM mass, which is velocity-dependent. This effect was studied at the example of the Debye mass, which was calculated in [40] and was shown to reproduce exactly the lattice data [90] (in contrast to a perturbative treatment, which is not gauge invariant and is about 50% off the data [90]). It is clear, that this CM dynamics is of a general character and

may be related to many features ascribed to QGP, for example to jet quenching, collective phenomena, and so on. This important topic requires a further careful investigation.

(4) What is the connection between deconfinement and Chiral Symmetry (CS) restoration? On the theoretical side, it was found in the FCM that the same correlator $D^E$, which ensures the CE confinement, enters the kernel of the nonlinear equation, the latter demonstrating Spontaneous Breaking of Chiral Symmetry (SBCS) [91]. Thus confinement entails SBCS, and both should disappear at the same temperature. This behaviour is observed in most of lattice simulations (see, for example, [92]). However, in some papers (for example, in [93]), a difference $\Delta T \sim 20$ MeV is found between the temperatures of the deconfinement and CS restoration, though it is not clear whether it is a physical effect or just a result of lattice approximations. One might inquire at this point of the role played by the CM confinement. This problem can be connected with the value of the chiral condensate $\langle \bar{q}q \rangle$, as a function of temperature. It used to be believed and found on the lattice that $\langle \bar{q}q \rangle$ disappeared for $T \geq T_c$. However, it was found recently, in new accurate calculations [94] for the quenched SU(2) case with overlap quarks (not violating CS), that almost a half of the $|\langle \bar{q}q \rangle|$ survives at $1.5T_c \geq T \geq T_c$. This observation calls for further work both on the lattice and in the analytic domain. In addition to the studies with quarks in the fundamental representation, discussed above, there appeared several works [95] on the phase transition for adjoint quarks, where it was found that $T_c < T_{SBCS}$. This fact stresses again that we are still far from the detailed understanding of the connection between confinement and SBCS.

(5) An important role in comparison of the QGP properties and results of RHIC experiments is played by the transport coefficient of the QGP, and especially by the shear viscosity $\eta$ and bulk viscosity $\zeta$ [96]. The existing calculations are not very reliable since they exploit nonperturbative dynamics in typically Minkowski (not Euclidean) configurations. The FCM, supplied by a careful analytic continuation from the Euclidean region, is able to produce both $\eta$ and $\zeta$ as saturated by propagators of two-gluon glueballs, coupled by the CM confinement. This work is in progress now.

(6) The FCM approach to the phase transition at nonzero $T$ and $\mu$ was given above, in section 5.1, based on the assumption that finite density does not affect strongly the vacuum energy gap, the latter being known from conformal anomaly. This is supported by lattice calculations [60] of the free energy $F(T,\mu)$ and looks plausible, since the internal scale of the vacuum energy density is connected to excitations with the mass of order of the lowest glueball mass, $M \approx 1.5$ GeV, whereas the corresponding $\mu$ is much lower. However, this question requires further detailed studies since it may change drastically the entire picture of the phase transition at low $T$'s due to density. Another point which might invalidate the standard picture of the $qq$ pairing phases is the fact that vacuum fields, especially measured by the CM correlators, are very strong and

can deform or totally destroy this pairing, preferring the $q\bar{q}$ pairing.

(7) A very important but still unresolved question is the dimensional transition from 4D to 3D with the temperature increase. Studying lattice data for the spacial string tension $\sigma_H(T)$ (see, for example, [97] and refs. therein), one can see a sharp change of its behaviour at $T = 1.5T_c$, for SU(2), and at $T = 1.2T_c$, for SU(3), which is not explained by theory. At larger $T$ one has a typical 3D behaviour $\sigma_H(T) \sim T^2$. The coefficient was considered, for example, in [98]. This point of almost "dimensional phase transition" deserves more study.

(8) There is an interesting development in the theory of the QGP, namely, QGP in an external field, which is totally beyond the scope of this review. We refer the reader to [99] and papers cited there for details.

(9) Finally, let us mention the problem of the phase transition from nuclear matter to quark matter. The EoS for the nuclear matter at growing density cannot be obtained as an extrapolation of the EoS for the normal nuclear density. As was mentioned in [81,83], density may strongly distort the usual confinement forces between quarks in a nucleon, the latter may loose in its mass and radius, and multiquark bags may be formated. This very interesting development may be of a practical use and can be connected both to the phenomenon of the so-called nuclear scaling [100] and to the hot point of quark stars — see, for example, [86].

We stop at this point leaving, however, many interesting problems beyond the scope of this review.

## Acknowledgements

This work was supported by the Federal Agency for Atomic Energy of Russian Federation, by the Federal Programme of the Russian Ministry of Industry, Science, and Technology No. 40.052.1.1.1112, by the grant NSh-4961.2008.2 for the leading scientific schools, and by the grants RFFI-06-02-17012 and RFFI-06-02-17120. Work of A. V. N. was supported by DFG-436 RUS 113/991/0-1(R), PTDC/FIS/70843/2006-Fisica, and by the non-profit "Dynasty" foundation and ICFPM. M. A. T. would like to acknowledge the partial support from the President Grant No. MK-2130.2008.2.

## References

1. B. Müller, J. L. Nagle, *Ann. Rev. Nucl. Part. Sci.* **56** (2006) 93; D. d'Enterria, *J. Phys. G* **34** (2007) S53; BRAHMS: *Nucl. Phys. A* **757** (2005) 1; PHENIX: *Nucl. Phys. A* **757** (2005) 184; PHOBOS: *Nucl. Phys. A* **757** (2005) 28; STAR: *Nucl. Phys. A* **757** (2005) 102.
2. J. Kapusta, *Finite Temperature Field theory* (Cambridge University Press, Cambridge, 1989); K.Yagi, T.Hatsuda and Y.Miake, *Quark-gluon Plasma* (Cambridge Univ. Press, Cambridge 2005).
3. G. J. Gross, R. D. Pisarski, and L. G. Yaffe, *Rev. Mod. Phys.* **53** (1981) 43; L. G. Yaffe, *Nucl. Phys. B (Proc. Suppl.)* **106** (2002) 117; M. Gyulassy and L. McLerran, *Nucl. Phys. A* **750** (2005) 30.

4. H. G. Dosch, *Phys. Lett. B* **190** (1987) 177; H. G. Dosch and Yu.A.Simonov, *Phys. Lett. B* **205** (1988), 339; Yu.A.Simonov, *Nucl. Phys. B* **307** (1988) 512.
5. A. Di Giacomo, H. G. Dosch, V. I. Shevchenko, and Yu. A. Simonov, *Phys. Rep.* **372** (2002) 319.
6. Yu. A. Simonov, *Proc. QCD: Perturbative or Nonperturbative* eds. L.Ferreira., P.Nogueira, J.I.Silva-Marcos (World Scientific, Singapore, 2001), p. 60; arXiv: hep-ph/9911327.
7. A. M. Badalian, V. I. Shevchenko, and Yu. A. Simonov, *Yad. Fiz.* **69** (2006) 1818.
8. M. D'Elia, A. Di Giacomo, and E. Meggiolaro, *Phys. Lett. B* **408** (1997) 315; *Phys. Rev. D* **67** (2003) 114504; A. Di Giacomo, E. Meggiolaro, and H. Panagopoulos, *Nucl. Phys. B* **483** (1997) 371.
9. Yu. A. Simonov, *JETP Lett.* **55** (1992) 605.
10. Yu. A. Simonov, *Proc. Varenna 1995, Selected Topics in Nonperturbative QCD*, p.319.
11. Yu. A. Simonov, *JETP Lett.* **54** (1991) 249.
12. Yu. A. Simonov, *Phys. At. Nucl.* **58** (1995) 309.
13. A. V. Nefediev and Yu. A. Simonov, *Phys. At. Nucl.* **71** (2008) 171.
14. Yu. A. Simonov and J. A. Tjon, *Ann. Phys.* **223** (1993) 1, *ibid* **300** (2002) 54.
15. M. Halpern, *Phys. Rev. D* **19** (1979) 517; I. Aref'eva, *Theor Math. Phys.* **43**, 353 (1980); N. Bralic, Phys. Rev. D **22** (1980) 3090; Yu. A. Simonov, *Sov. J. Nucl. Phys.* **50** (1989) 134; M. Hirayama and S. Matsubara, *Progr. Theor. Phys.* **99** (1998) 691.
16. Yu. A. Simonov, *JETP Lett.* **71** (2000) 127; V. I. Shevchenko and Yu. A. Simonov, *Phys. Rev. Lett.* **85** (2000) 1811.
17. Yu. A. Simonov, *Z. Phys. C* **53** (1992) 419; A. M. Badalian, B. L. G. Bakker, and Yu. A. Simonov, *Phys. Rev. D* **75** (2007) 116001.
18. Y. Koma and M. Koma, *Nucl. Phys. B* **769** (2007) 79.
19. A. M. Badalian, A. V. Nefediev, and Yu. A. Simonov, *JETP Lett.* **88** (2008) 648.
20. L. Brink, P. Di Vecchia, and P. Howe, *Nucl. Phys. B* **118** (1977) 76.
21. A. Yu. Dubin, A. B. Kaidalov, and Yu. A. Simonov, *Phys. Lett. B* **323** (1994) 41.
22. Yu. S. Kalashnikova and A. V. Nefediev, *Phys. At. Nucl.* **60** (1997) 1389.
23. Yu. A. Simonov, *Phys. Lett. B* **226** (1989) 151.
24. P. A. M. Dirac, *Letures on Quantum Mechanics* (Belter Graduate School of Science, Yeshiva University, New York (1964)).
25. V. L. Morgunov, A. V. Nefediev, and Yu. A. Simonov, *Phys. Lett. B* **459** (1999) 653.
26. Yu. S. Kalashnikova, A. V. Nefediev, and Yu. A. Simonov, *Phys. Rev. D* **64** (2001) 014037.
27. E. Eichten and F. L. Feinberg, *Phys. Rev. D* **23** (1981) 2724.
28. Yu. A. Simonov, *Nucl. Phys. B* **324** (1989) 67; A. M. Badalian and Yu. A. Simonov, *Phys. Atom. Nucl.* **59**, (1996) 2164, [*Yad. Fiz.* **59** (1996) 2247]; M. Schiestl and H. G. Dosch, *Phys. Lett. B* **209** (1988) 85.
29. A. Barchielli, N. Brambilla, and G. M. Prosperi, *Nuovo Cim. A* **103** (1990) 59; A. Pineda and A. Vairo, *Phys. Rev. D* **63** (2001) 054007; N. Brambilla and A. Vairo, *Phys. Rev. D* **55** (1997) 3974.
30. D. Gromes, *Z. Phys. C* **26** (1984) 401.
31. A. M. Badalian, A. V. Nefediev, and Yu. A. Simonov, *Phys. Rev. D* **78** (2008) 114020.
32. Yu. A. Simonov, in: *"Sense of Beauty in Physics"* (Pisa Univ. Press, 2006), p.29; A. M. Badalian and Yu. A. Simonov, *Yad. Phys.* **59** (1996) 2247.
33. S. Gupta, K. Hübner, and O. Kaczmarek, *Nucl. Phys. A* **785** (2007) 278; K. Hübner and C. Pica, arXiv:0809.3933[hep-lat].
34. Yu. A. Simonov, *Phys. At. Nucl.* **58** (1995) 107; *ibid* **65** (2002) 135.

35. Yu. A. Simonov, *Ann. Phys.* **323** (2008) 783.
36. E. V. Komarov and Yu. A. Simonov, *Ann. Phys.* **323** (2008) 1230.
37. H. G. Dosch, H.-J. Pirner, and Yu. A. Simonov, Phys.Lett. B **349** (1995) 335.
38. G. S. Bali, *Phys. Rev. D* **62** (2000) 114503; S. Deldar, *Phys. Rev. D* **62** (2000) 034509.
39. Yu. A. Simonov, *Phys. At. Nucl.* **70** (2007) 44.
40. N. O. Agasian and Yu. A. Simonov, *Phys. Lett. B* **639** (2006) 82.
41. Yu. A. Simonov, *Nucl. Phys. B* **592** (2001) 350.
42. Yu. A. Simonov, *Phys. Lett. B* **619** (2005) 293.
43. O. Kaczmarek, F. Karsch, P. Petreczky, and F. Zantow, *Phys. Lett. B* **543** (2002) 41.
44. Yu. A. Simonov, *Phys. At. Nucl.* **69** (2006) 528.
45. O. Kaczmarek and F. Zantow, arXiv:hep-lat/0506019.
46. A. Di Giacomo *et al.*, *Phys. At. Nucl.* **70** (2007) 908.
47. F. Karsch, *J. Phys. Conf. Ser.* **46** (2006) 122.
48. C. Bernard, T. Burch, C. DeTar, S. Gottlieb, L. Levkova, U. M. Heller, J. E. Hetrick, D. B. Renner, D. Toussaint, and R. Sugar, *PoSLAT2006* **139** (2006).
49. Yu. A. Simonov and M. A. Trusov, *Phys. Lett. B* **650** (2007) 36; *JETP Lett.* **85** (2007) 730.
50. F. Karsch, arXiv:hep-ph/0701210.
51. Y. Aoki, Z. Fodor ,S. D. Katz, K. K. Szabo, *JHEP* **0601** (2006) 089.
52. P.Petreczky, hep-lat/0409139; *Nucl. Phys. A* **785** (2007) 10.
53. E. V. Shuryak and I. Zahed, *Phys. Rev. D* **70** (2004) 054507.
54. K. Hübner, O. Kaczmarek, F. Karsch, and O. Vogt, arXiv:hep-lat/0408031.
55. F. Buisseret and C. Semay, *Phys. Rev. D* **70** (2004) 077501.
56. A. B. Migdal, D. N. Voskresenksy, and V. S. Popov, *Pis'ma v ZhETF*, **24** (1976) 186; *ZhETF*, **72** (1977) 834.
57. Yu. A. Simonov, *Phys. Atom. Nucl.* **68** (2005) 709.
58. D. Antonov, S. Domdey, and H.-J. Pirner, *Nucl. Phys. A* **789** (2007) 357.
59. M. D'Elia, A. Di Giacomo and E. Meggiolaro, *Phys. Rev. D* **67** (2003) 114504.
60. M. Döring, S. Ejiri, O. Kaczmarek, F. Karsch, E. Laermann, *Eur. Phys. J. C* **46** (2006) 179.
61. M. P. Lombardo, *PoSCPOD2006* (2006) 003; M. D. 'Elia and M. P. Lombardo, *Phys. Rev. D* **67** (2003) 014505, ibid **70** (2004) 074509; Ph. de Forcrand and O.Philipsen, *Nucl. Phys. B* **673** (2003) 170.
62. M. Shifman, A. Vainshtein, V. Zakharov, *Nucl. Phys. B* **147** (1979) 385, 448.
63. Yu. A. Simonov, *Phys. At. Nucl.* **69** (2006) 528.
64. F. Karsch, Prog. Theor. Phys. Suppl. **153** (2004) 106.
65. C. Schmidt, hep-lat/0701019; C. Bernard *et al.*, *Phys. Rev. D* **75** (2007) 094505; R. Gavai, *Pramana67* (2006) 885; U. M. Heller, *PoSLAT2006* (2006) 011; F. Karsch, hep-lat/0601013, *J. Phys. Conf. Ser.* **46** (2006) 122.
66. S. Aoki, *Int. J. Mod. Phys. A* **21** (2006) 682.
67. C. R. Allton, S. Ejiri, S. J. Hands, *et al.*, *Nucl. Phys. Proc. Suppl.* **141** (2005) 186; Nucl. Phys. Proc. Suppl. **141** (2008) 186.
68. Z. Fodor, S. D. Katz, C. Schmidt, JHEP **0703** (2007) 121.
69. M. Stephanov, *PoSLAT2006* (2006) 024.
70. A. Di Giacomo, *Braz. J. Phys.* **37** (2007) 208.
71. V. G. Bornyakov *et al.*, *PoSLAT2005* (2005) 157.
72. D. Gross, R. D. Pisarski, L. G. Yaffe, *Rev. Mod. Phys.* **53** (1981) 43.
73. L. Mc Lerran and B.Svetitsky, *Phys. Lett. B* **98** (1981) 195.
74. N. Weiss, *Phys. Rev. D* **24** (1981) 475, *ibid* **25** (1982) 2667.

75. M. Ogilvie amd P. N. Meisinger, arXiv:0811.2025[hep-lat].
76. K. Fukushima, *Phys. Lett. B* **553** (2003) 38; *Phys. Rev. D* **68** (2003) 045004; *Phys. Lett. B* **591** (2004) 277; Y. Hatta and K. Fukushima, *Phys. Rev. D* **69** (2004) 097502.
77. C. Sasaki, B. Friman, K. Redlich, *Phys. Rev. D* **75** (2007) 054026 (2007); S. Rössner, T. Hell, C. Ratti, and W. Weise, arXiv:0712.3152[hep-ph]; S. K. Ghosh, T. K. Mukherjee, M. G. Mustafa, and R. Ray, arXiv:0805.4690.
78. A. Peshier, *Phys. Rev. D* **70** (2004) 034016; *J. Phys. G* **31** (2005) 5371.
79. W. Cassing, *Nucl. Phys. A* **791** (2007) 365.
80. N. O. Agasian, *JETP Lett.* **57** (1993) 208; N. O. Agasian, D. Ebert, and E. Ilgenfritz, *Nucl. Phys. A* **637** (1998) 135.
81. Yu. A. Simonov, arXiv:hep-ph/0605022; Yu. A. Simonov and M. A. Trusov (in preparation).
82. see *e.g.* F. Wilczek and K. Rajagopal, in “At the Frontier of Particla Physics. Handbook of QCD”, v. 3, ed. M.Shifman (World Scientific, Singapore, 2001); B. O. Kerbikov, *Phys. Rev. D* **70** (2004) 057503; *Phys. At. Nucl.* **68** (2005) 916.
83. N. O. Agasian, B. O. Kerbikov, and V. I. Shevchenko, *Phys. Rept.* **320** (1999) 131.
84. M. Döring *et al.*, *Phys. Rev. D* **75** (2007) 054504; G. Aarts *et al.*, *Phys. Rev. D.* **76** (2007) 094513.
85. N. K. Glendenning, *Phys. Rev. D* **46** (1992) 1274; F. Özel, *Nature* **441** (2006) 1115; G. H. Bordbar, M. Bigdeli, and T. Yazdizadeh, *Int. J. Mod. Phys. A* **21** (2006) 5991.
86. M. Alford *et al.*, *Nature* **445** (2007) E7.
87. I. M. Dremin, *Eur. Phys. J. C* **56** (2008) 81; I. M. Dremin *et al.*, arXiv:0809.2472[nucl-th].
88. Yu. A. Simonov, *JETP Lett.* **55** (1992) 605; E. L. Gubankova and Yu. A. Simonov, *Phys. Lett. B* **360** (1995) 93; N. O. Agasian, *JETP Lett.* **57** (1993) 208.
89. Yu. A. Simonov, *Nucl. Phys. B* **324** (1989) 67; Yu. A. Simonov, in ”Sense of Beauty in Physics”, volume in honor of Adriano Di Giacomo, Pisa univ. Press, p.29, 2006.
90. O. Kaczmarek and F. Zantow, *Phys. Rev. D* **71** (2005) 114510.
91. Yu. A. Simonov, *Phys. At. Nucl.* **60** (1997) 2069; *Phys. Rev. D* **65** (2002) 094018.
92. F.Karsch, *PoSCPOD07* (2007) 026, *PoSLAT2007* (2007) 015 and refs. therein.
93. Z. Fodor, *PoSLAT2007* (2007) 011.
94. P. Buividovich, E. Lushchevskaya, M. Polikarpov, *Phys. Rev. D* **78** (2008) 074505.
95. F. Karsch, M. Lutgemeier, *Nucl. Phys. B* **550** (1999) 449; G. Cossu *et.al.*, *Phys. Rev. D* **77** (2008) 074506; J. Engels, S. Holtmann, and T. Schulze, *Nucl. Phys. B* **724** (2005) 357.
96. see *e.g.* H. Meyer, arXiv:0809.5202[hep-lat].
97. N. O. Agasian, *Phys. Lett. B* **562** (2003) 257.
98. V. P. Nair, arXiv:hep-th/0309061; *Nucl. Phys. B* **691** (2004) 182.
99. N. O. Agasian and S. M. Fedorov, *Phys. Lett. B* **663** (2008) 445; N. O. Agasian, *Phys. At. Nucl.* **71** (2008) 1967.
100. A. M. Baldin, *Short Communications in Physics*, *Lebedev Institute for Physics* **1** (1971) 35; Yu. D. Bayukov *et al.*, *Izvestia Akad. Nauk SSSR, Fizika* **30** (1966) 521; *Yad. Fiz.* **18** (1973) 1246.